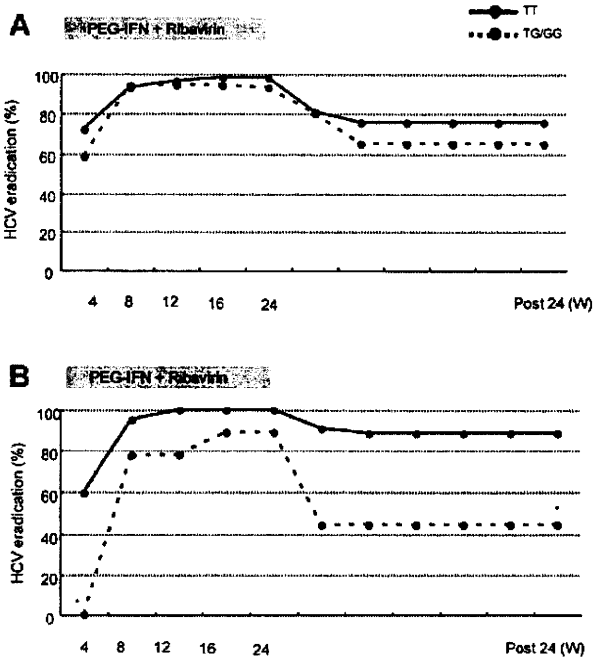

Fig. 1. Changes over time in virological response rates were confirmed in patients treated with PEG-IFN plus RBV, and the time courses were analyzed after separating the patients infected with genotypes 2a and 2b. Patients with the IL28B major (TT allele) are indicated in the figure by a continuous line and those with IL28B hetero or minor (TG or GG), by a dotted line. IL28B-TG and -GG patients showed significantly lower rates of rapid and sustained virological response, compared to IL28B-TT patients. *P*-values were two-tailed and those of less than 0.05 were considered to be statistically significant. $^{*}P < 0.01$.

Among the eight patients who withdrew from both drugs, four, including one who stopped at week 7, had achieved a sustained virological response. Among four patients who withdrew from RBV alone, three had achieved a sustained virological response. The events leading to drug withdrawal were HCC treatment (n = 2), general fatigue (n = 2), retinopathy, neuro-psychiatric event, severe dermatological symptoms suggestive of the drug-induced hypersensitivity syndrome, and arrhythmia.

DISCUSSION

Recent studies suggest that genetic variations in IL28B are strongly associated with response to therapy of chronic HCV infection with genotype 1 [Ge et al., 2009; Suppiah et al., 2009; Tanaka et al., 2009] and with spontaneous HCV clearance [Thomas et al., 2009]. In this study, univariate analyses showed that the sustained virological response was correlated significantly with IL28B polymorphism (rs8099917) as well as age, adherence to RBV and rapid virological response, and multiple logistic-regression analysis showed that only a rapid virological response was associated with a sustained virological response in all patients infected with genotype 2 (Table V). Although the IL28B polymorphisms are not so useful for predicting the clinical outcomes of PEG-IFN plus RBV combination therapy among patients with genotype 2, compared to genotype 1, IL28B polymorphism was predictive of PEG-IFN plus RBV treatment outcomes among patients with genotype 2 and, more remarkably, among patients with genotype 2b in this study. Indeed, both rapid and sustained virological response rates according to the rs8099917 genotypes were different significantly in patients with genotype 2b but not in patients with genotype 2a. Furthermore, in the plot of virological response (Fig. 1), a stronger effect of the IL28B allele was observed in patients with genotype 2b than with genotype 2a.

It has been reported that there was no significant association between genetic variation in IL28B and response to therapy of HCV patients infected with genotype 2 or 3, indicating that the prognostic value of the risk allele for treatment response might be limited to individuals with difficult-to-treat HCV genotypes [Rauch et al., 2010]. This report lacks details of the distribution of the various genotypes. The present study agrees with a more recent report that the IL28B polymorphism was associated with a sustained virological response in patients with chronic HCV infection with genotype 2 or 3 who did not achieve a rapid virological response [Mangia et al., 2010]. In Japan, the percentage of HCV infection with genotype 1b is 70%, genotype 2a is 20% and genotype 2b is 10%, whilst other genotypes are observed only rarely. In this study, the association of IL28B polymorphism with response to therapy was analyzed in more detail, considering the subtypes 2a and 2b, and IL28B polymorphism (rs8099917) found to be linked more closely to the virological response of patients infected with genotype 2b than those with genotype 2a. A recent in vitro study, which constructed several chimeric virus clones between HCV-2b and HCV-JFH1 (2a), also supported subgenotypic differences between genotype 2a and 2b [Suda et al., 2010]. The authors speculated that the prognostic value of the risk allele for treatment response might be more pronounced in individuals with difficult-to-treat HCV subgenotypes, such as patients infected with genotype 2b, compared with 2a. In addition, the prevalence of the IL28B minor allele is much higher in Caucasians and African Americans than in eastern Asian populations [Thomas et al., 2009], which suggest that the effects of IL28B polymorphism could be more pronounced in non-Asian populations. In the present results, however, the sustained virological response rate of patients infected with genotype 2b was higher than that of patients with genotype 2a overall. We speculate that, among patients infected with genotype 2b, only those with the IL28B minor variant might be treatment-refractory. That possibility might be validated further by a larger cohort study with genotype 2b.

The sustained virological response rates decreased significantly with failure of adherence to RBV (Table III), which was extracted as a factor associated with sustained virological response by univariate

analysis (Table IV). Regardless of the drug adherence, end of treatment response rates of patients infected with genotype 2 were around 94–99%, but the sustained virological response rates of the patients who received a total cumulative treatment dose of RBV of <80% was reduced significantly. As reported previously, increased RBV exposure during the treatment phase was associated with an increased likelihood of a sustained virological response [McHutchison et al., 2009] and these results confirm the importance of RBV in order to prevent relapse. Furthermore, host genetic variation leading to inosine triphosphatase (ITPA) deficiency protects against hemolytic anemia in chronic hepatitis C patients receiving RBV as revealed recently [Fellay et al., 2010]. We have reported also that the *ITPA* SNP, rs1127354, is confirmed to be a useful predictor of RBV-induced anemia in Japanese patients and that the incidence of early dose reduction was significantly higher in patients with ITPA-major (CC) variant as expected and, more importantly, that a significant higher sustained virological response rate was achieved in patients with the *ITPA-hetero*/minor (CA/AA) variant with non-genotype 1 or low viral loads [Sakamoto et al., 2010].

A rapid virological response was extracted in this study as a factor associated with sustained virological response only by multivariate analysis. It has been reported recently that a rapid virological response is an important treatment predictor and that drug adherence, which is reported to affect the therapeutic efficacy in patients infected with genotype 1, had no impact on the both sustained and rapid virological responses in combination therapy for patients infected with genotype 2 [Inoue et al., 2010]. The reasons why several host factors useful for predicting the response to therapy in patients with genotype 1, such as gender, age, progression of liver fibrosis and IL28B polymorphism had no influence on the efficacy in patients with genotype 2, can be attributed to IFN-sensitive genotypes. Similarly, the other viral factors useful for predicting the response to therapy, such as viral load and amino acid substitutions in the Core and NS5A regions had no influence on treatment outcomes. In this study, patients who achieved a rapid virological response had a high sustained virological response rate, regardless of IL28B polymorphism in patients with genotype 2a but, interestingly, none of the IL28B-TG and -GG patients with genotype 2b achieved a sustained virological response (although there were nine IL28B-TG and -GG patients with genotype 2b, two could not be determined as rapid virological response because the times at which they became HCV-negative were not recorded clearly, being described as 4–8 weeks.) These results also suggest that patients with both genotype 2b and IL28B minor allele are refractory cases.

IL28B encodes a protein also known as IFN-λ3 [O'Brien, 2009]. *IL28A* (IFN-λ2) and *IL29* (IFN-λ1) are found adjacent to *IL28B* on chromosome 19. These three IFN-λ cytokines, discovered in 2003 by two independent groups [Kotenko et al., 2003; Sheppard et al., 2003] have been suggested to be involved in the suppression of replication of a number of viruses, including HCV [Robek et al., 2005; Marcello et al., 2006; Tanaka et al., 2010]. Humans have these three genes for IFN-λ, and this group of cytokines is now collectively referred to as type III IFN [Zhou et al., 2007]. IFN-λ functionally resembles type I IFN, inducing antiviral protection in vitro [Kotenko et al., 2003; Sheppard et al., 2003] as well as in vivo [Ank et al., 2006]. Type III IFN utilizes a receptor complex different from that of type I IFN, but both types of IFN induce STAT1, STAT2, and STAT3 activation by activation of a highly overlapping set of transcription factors, and the two types of IFN seem to have similar biological effects at a cellular level. Some in vitro studies have suggested that IFN-α induces expression of IFN-λ genes [Siren et al., 2005]. Other in vitro studies also suggest that IFN-λ inhibits hepatitis C virus replication through a pattern of signal transduction and regulation of interferon-stimulated genes that is distinct from IFN-α and that the anti-HCV activity of either IFN-α or IFN-λ is enhanced by a low dose of the other [Marcello et al., 2006]. A novel mechanism of the interaction between IFN-α and IFN-λ may play a key role in the suppression of HCV [O'Brien, 2009].

In conclusion, IL28B polymorphism is predictive of PEG-IFN plus RBV treatment outcomes in patients infected with genotype 2, and more remarkably with genotype 2b. These results suggest that IL-28B polymorphism affects responses to IFN-based treatment in more difficult-to-treat subpopulations of HCV patients, and that intersubgenotypic differences between genotype 2a and 2b are revealed by responses to PEG-IFN plus RBV treatment according to IL28B variants.

ACKNOWLEDGMENTS

The study is based on 10 multicenter hospitals throughout Japan, in the Kanto area (Tokyo Medical and Dental University Hospital, Musashino Red Cross Hospital, Kashiwa City Hospital, Kudanzaka Hospital, Showa General Hospital, Tsuchiura Kyodo General Hospital, Toride Kyodo General Hospital), Tokai area (Nagoya City University Hospital, Mishima Social Insurance Hospital) and Chugoku/Shikoku area (Ehime University Hospital).

REFERENCES

Alter MJ. 1997. Epidemiology of hepatitis C. Hepatology 26:62S–65S.

Ank N, West H, Bartholdy C, Eriksson K, Thomsen AR, Paludan SR. 2006. Lambda interferon (IFN-lambda), a type III IFN, is induced by viruses and IFNs and displays potent antiviral activity against select virus infections in vivo. J Virol 80:4501–4509.

Fellay J, Thompson AJ, Ge DL, Gumbs CE, Urban TJ, Shianna KV, Little LD, Qiu P, Bertelsen AH, Watson M, Warner A, Muir AJ, Brass C, Albrecht J, Sulkowski M, McHutchison JG, Goldstein DB. 2010. ITPA gene variants protect against anaemia in patients treated for chronic hepatitis C. Nature 464:405–408.

Fried MW, Shiffman ML, Reddy KR, Smith C, Marinos G, Goncales FL, Haussinger D, Diago M, Carosi G, Dhumeaux D, Craxi A, Lin A, Hoffman J, Yu J. 2002. Peginterferon alfa-2a plus ribavirin for chronic hepatitis C virus infection. N Engl J Med 347:975–982.

Ge D, Fellay J, Thompson AJ, Simon JS, Shianna KV, Urban TJ, Heinzen EL, Qiu P, Bertelsen AH, Muir AJ, Sulkowski M, McHutchison JG, Goldstein DB. 2009. Genetic variation in IL28B predicts hepatitis C treatment-induced viral clearance. Nature 461:399–401.

Hoofnagle JH. 1994. Therapy of acute and chronic viral hepatitis. Adv Intern Med 39:241–275.

Inoue Y, Hiramatsu N, Oze T, Yakushijin T, Mochizuki K, Hagiwara H, Oshita M, Mita E, Fukui H, Inada M, Tamura S, Yoshihara H, Hayashi E, Inoue A, Imai Y, Kato M, Miyagi T, Hohsui A, Ishida H, Kiso S, Kanto T, Kasahara A, Takehara T, Hayashi N. 2010. Factors affecting efficacy in patients with genotype 2 chronic hepatitis C treated by pegylated interferon alpha-2b and ribavirin: Reducing drug doses has no impact on rapid and sustained virological responses. J Viral Hepat 17:336–344.

Kotenko SV, Gallagher G, Baurin VV, Lewis-Antes A, Shen M, Shah NK, Langer JA, Sheikh F, Dickensheets H, Donnelly RP. 2003. IFN-lambdas mediate antiviral protection through a distinct class II cytokine receptor complex. Nat Immunol 4:69–77.

Mangia A, Thompson AJ, Santoro R, Piazzolla V, Tillmann HL, Patel K, Shianna KV, Mottola L, Petruzzellis D, Bacca D, Carretta V, Minerva N, Goldstein DB, McHutchison JG. 2010. An IL28B polymorphism determines treatment response of hepatitis C virus genotype 2 or 3 patients who do not achieve a rapid virologic response. Gastroenterology 139:821–827.

Marcello T, Grakoui A, Barba-Spaeth G, Machlin ES, Kotenko SV, MacDonald MR, Rice CM. 2006. Interferons alpha and lambda inhibit hepatitis C virus replication with distinct signal transduction and gene regulation kinetics. Gastroenterology 131:1887–1898.

McHutchison JG, Lawitz EJ, Shiffman ML, Muir AJ, Galler GW, McCone J, Nyberg LM, Lee WM, Ghalib RH, Schiff ER, Galati JS, Bacon BR, Davis MN, Mukhopadhyay P, Koury K, Noviello S, Pedicone LD, Brass CA, Albrecht JK, Sulkowski MS. 2009. Peginterferon alfa-2b or alfa-2a with ribavirin for treatment of hepatitis C infection. N Engl J Med 361:580–593.

O'Brien TR. 2009. Interferon-alfa, interferon-lambda and hepatitis C. Nat Genet 41:1048–1050.

Rauch A, Kutalik Z, Descombes P, Cai T, di Iulio J, Mueller T, Bochud M, Battegay M, Bernasconi E, Borovicka J, Colombo S, Cerny A, Dufour JF, Furrer H, Gunthard HF, Heim M, Hirschel B, Malinverni R, Moradpour D, Mullhaupt B, Witteck A, Beckmann JS, Berg T, Bergmann S, Negro F, Telenti A, Bochud PY. 2010. Genetic variation in IL28B is associated with chronic hepatitis C and treatment failure—A genome-wide association study. Gastroenterology 138:1240–1243.

Robek MD, Boyd BS, Chisari FV. 2005. Lambda interferon inhibits hepatitis B and C virus replication. J Virol 79:3851–3854.

Rosen HR, Gretch DR. 1999. Hepatitis C virus: Current understanding and prospects for future therapies. Mol Med Today 5:393–399.

Sakamoto N, Watanabe M. 2009. New therapeutic approaches to hepatitis C virus. J Gastroenterol 44:643–649.

Sakamoto N, Tanaka Y, Nakagawa M, Yatsuhashi H, Nishiguchi S, Enomoto N, Azuma S, Nishimura-Sakurai Y, Kakinuma S, Nishida N, Tokunaga K, Honda M, Ito K, Mizokami M, Watanabe M. 2010. ITPA gene variant protects against anemia induced by pegylated interferon-alpha and ribavirin therapy for Japanese patients with chronic hepatitis C. Hepatol Res 40:1063–1071.

Sheppard P, Kindsvogel W, Xu W, Henderson K, Schlutsmeyer S, Whitmore TE, Kuestner R, Garrigues U, Birks C, Roraback J, Ostrander C, Dong D, Shin J, Presnell S, Fox B, Haldeman B, Cooper E, Taft D, Gilbert T, Grant FJ, Tackett M, Krivan W, McKnight G, Clegg C, Foster D, Klucher KM. 2003. IL-28, IL-29 and their class II cytokine receptor IL-28R. Nat Immunol 4:63–68.

Siren J, Pirhonen J, Julkunen I, Matikainen S. 2005. IFN-alpha regulates TLR-dependent gene expression of IFN-alpha, IFN-beta, IL-28, and IL-29. J Immunol 174:1932–1937.

Suda G, Sakamoto N, Itsui Y, Nakagawa M, Mishima K, Onuki-Karakama Y, Yamamoto M, Funaoka Y, Watanabe T, Kiyohashi K, Nitta S, Azuma S, Kakinuma S, Tsuchiya K, Imamura M, Hiraga N, Chayama K, Watanabe M. 2010. IL-6-mediated intersubgenotypic variation of interferon sensitivity in hepatitis C virus genotype 2a/2b chimeric clones. Virology 407:80–90.

Suppiah V, Moldovan M, Ahlenstiel G, Berg T, Weltman M, Abate ML, Bassendine M, Spengler U, Dore GJ, Powell E, Riordan S, Sheridan D, Smedile A, Fragomeli V, Muller T, Bahlo M, Stewart GJ, Booth DR, George J. 2009. IL28B is associated with response to chronic hepatitis C interferon-alpha and ribavirin therapy. Nat Genet 41:1100–1104.

Tanaka Y, Nishida N, Sugiyama M, Kurosaki M, Matsuura K, Sakamoto N, Nakagawa M, Korenaga M, Hino K, Hige S, Ito Y, Mita E, Tanaka E, Mochida S, Murawaki Y, Honda M, Sakai A, Hiasa Y, Nishiguchi S, Koike A, Sakaida I, Imamura M, Ito K, Yano K, Masaki N, Sugauchi F, Izumi N, Tokunaga K, Mizokami M. 2009. Genome-wide association of IL28B with response to pegylated interferon-alpha and ribavirin therapy for chronic hepatitis C. Nat Genet 41:1105–1109.

Tanaka Y, Nishida N, Sugiyama M, Tokunaga K, Mizokami M. 2010. Lambda-Interferons and the single nucleotide polymorphisms: A milestone to tailor-made therapy for chronic hepatitis C. Hepatol Res 40:449–460.

Thomas DL, Thio CL, Martin MP, Qi Y, Ge D, O'Huigin C, Kidd J, Kidd K, Khakoo SI, Alexander G, Goedert JJ, Kirk GD, Donfield SM, Rosen HR, Tobler LH, Busch MP, McHutchison JG, Goldstein DB, Carrington M. 2009. Genetic variation in IL28B and spontaneous clearance of hepatitis C virus. Nature 461:798–801.

Zeuzem S, Feinman SV, Rasenack J, Heathcote EJ, Lai MY, Gane E, O'Grady J, Reichen J, Diago M, Lin A, Hoffman J, Brunda MJ. 2000. Peginterferon alfa-2a in patients with chronic hepatitis C. N Engl J Med 343:1666–1672.

Zhou Z, Hamming OJ, Ank N, Paludan SR, Nielsen AL, Hartmann R. 2007. Type III interferon (IFN) induces a type I IFN-like response in a restricted subset of cells through signaling pathways involving both the Jak-STAT pathway and the mitogen-activated protein kinases. J Virol 81:7749–7758.

Journal of Medical Virology 83:445–452 (2011)

Sequences in the Interferon Sensitivity-Determining Region and Core Region of Hepatitis C Virus Impact Pretreatment Prediction of Response to PEG-Interferon Plus Ribavirin: Data Mining Analysis

Masayuki Kurosaki,[1] Naoya Sakamoto,[2] Manabu Iwasaki,[3] Minoru Sakamoto,[4] Yoshiyuki Suzuki,[5] Naoki Hiramatsu,[6] Fuminaka Sugauchi,[7] Akihiro Tamori,[8] Mina Nakagawa,[2] and Namiki Izumi, MD[1]*

[1]*Division of Gastroenterology and Hepatology, Musashino Red Cross Hospital, Tokyo, Japan*
[2]*Department of Gastroenterology and Hepatology, Tokyo Medical and Dental University, Tokyo, Japan*
[3]*Department of Computer and Information Science, Seikei University, Tokyo, Japan*
[4]*First Department of Internal Medicine, University of Yamanashi, Yamanashi, Japan*
[5]*Department of Hepatology, Toranomon Hospital, Tokyo, Japan*
[6]*Department of Gastroenterology and Hepatology, Osaka University Graduate School of Medicine, Osaka, Japan*
[7]*Department of Gastroenterology and Metabolism, Nagoya City University Graduate School of Medical Sciences, Aichi, Japan*
[8]*Department of Hepatology, Osaka City University Medical School, Osaka, Japan*

The aim of the present study was to clarify the significance of viral factors for pretreatment prediction of sustained virological response to pegylated-interferon (PEG-IFN) plus ribavirin (RBV) therapy for chronic hepatitis C using data mining analysis. Substitutions in the IFN sensitivity-determining region (ISDR) and at position 70 of the HCV core region (Core70) were determined in 505 patients with genotype 1b chronic hepatitis C treated with PEG-IFN plus RBV. Data mining analysis was used to build a predictive model of sustained virological response in patients selected randomly (n = 304). The reproducibility of the model was validated in the remaining 201 patients. Substitutions in ISDR (odds ratio = 9.92, $P < 0.0001$) and Core70 (odds ratio = 1.92, $P = 0.01$) predicted sustained virological response independent of other covariates. The decision-tree model revealed that the rate of sustained virological response was highest (83%) in patients with two or more substitutions in ISDR. The overall rate of sustained virological response was 44% in patients with a low number of substitutions in ISDR (0–1) but was 83% in selected subgroups of younger patients (<60 years), wild-type sequence at Core70, and higher level of low-density lipoprotein cholesterol (LDL-C) (≥120 mg/dl). Reproducibility of the model was validated ($r^2 = 0.94$, $P < 0.001$). In conclusion, substitutions in ISDR and Core70 of HCV are significant predictors of response to PEG-IFN plus RBV therapy. A decision-tree model that includes these viral factors as predictors could identify patients with a high probability of sustained virological response. ***J. Med. Virol. 83:445–452, 2011.***

KEY WORDS: data mining; decision-tree model; ISDR; core region; PEG-interferon

INTRODUCTION

The combination of pegylated-interferon (PEG-IFN) plus ribavirin (RBV) is currently the most effective therapy for chronic hepatitis C, but the rate of sustained virological response after 48 weeks of therapy is about 50% in patients with HCV genotype 1b and a high HCV

Grant sponsor: Ministry of Health, Labor and Welfare, Japan.
The authors report no conflicts of interest.

*Correspondence to: Namiki Izumi, MD, Division of Gastroenterology and Hepatology, Musashino Red Cross Hospital, 1-26-1 Kyonan-cho, Musashino-shi, Tokyo 180-8610, Japan. E-mail: nizumi@musashino.jrc.or.jp

Accepted 26 October 2010
DOI 10.1002/jmv.22005
Published online in Wiley Online Library (wileyonlinelibrary.com).

RNA titer [Manns et al., 2001; Fried et al., 2002]. The most reliable means to predict sustained virological response is to monitor the viral response during the early weeks of treatment. The early virological response, defined as undetectable HCV RNA at week 12, is associated with a high rate of sustained virological response [Davis et al., 2003; Lee and Ferenci, 2008]. The rapid virological response, defined as undetectable HCV RNA at week 4 of therapy, is even more predictive of sustained virological response than the early virological response [Jensen et al., 2006; Yu et al., 2008; Izumi et al., 2010]. However, there is no established means that predicts the virological response before commencing treatment. Recent reports have revealed that single nucleotide polymorphisms located near the *IL28B* gene show a strong association with the response to PEG-IFN plus RBV therapy [Ge et al., 2009; Suppiah et al., 2009; Tanaka et al., 2009; Kurosaki et al., 2010c]. These findings indicate that the host factor is an important determinant of the treatment response. On the other hand, the present study's authors have reported that a stretch of 40 amino acids in the NS5A region of HCV, designated as the interferon sensitivity-determining region (ISDR), has a close association with the virological response to interferon mono-therapy [Enomoto et al., 1995, 1996; Kurosaki et al., 1997]. More recently, amino acid substitutions at positions 70 and 91 of the core region have been reported to be associated with response to PEG-IFN plus RBV combination therapy [Akuta et al., 2005, 2007a]. The impact of these HCV substitutions on treatment response is yet to be validated.

Decision-tree analysis is a core component of data mining analysis that can be used to build predictive models [Breiman et al., 1980]. This method has been used to define prognostic factors in various diseases such as prostate cancer [Garzotto et al., 2005], diabetes [Miyaki et al., 2002], melanoma [Averbook et al., 2002; Leiter et al., 2004], colorectal carcinoma [Zlobec et al., 2005; Valera et al., 2007], and liver failure [Baquerizo et al., 2003]. The major advantage of decision-tree analysis over logistic regression analysis is that the results of analysis are easy to understand. The simple allocation of patients into subgroups by following the flowchart form could define the predicted possibility of outcome [LeBlanc and Crowley, 1995].

Decision-tree analysis was used for the prediction of early virological response (undetectable HCV RNA within 12 weeks of therapy) to PEG-IFN and RBV combination therapy in chronic hepatitis C [Kurosaki et al., 2010a], and more recently for the pretreatment prediction of sustained virological response [Kurosaki et al., 2010b]. In the latter model, simple and noninvasive standard tests were used as parameters; specialized tests such as viral mutations and host genetics, or invasive tests such as liver histology, were not included because the aim of that model was for use in general medical practice, especially in some countries or areas where resources are limited. Thus, the impact of viral mutations or liver histology was not considered in that model.

The present study examined whether including viral substitutions in ISDR and the core region of HCV in the decision-tree model could improve its predictive accuracy over the previous model to identify chronic hepatitis C patients who are likely to respond to PEG-IFN plus RBV therapy.

MATERIALS AND METHODS

Patients

This multicenter retrospective cohort study included 505 chronic hepatitis C patients who were treated with PEG-IFN alpha-2b and RBV at Musashino Red Cross Hospital, Toranomon Hospital, Tokyo Medical and Dental University, Osaka University, Nagoya City University Graduate School of Medical Sciences, Yamanashi University, Osaka City University, and their related hospitals. The inclusion criteria were: (1) genotype 1b, (2) HCV RNA titer higher than 100 kIU/ml by quantitative PCR (Cobas Amplicor HCV Monitor v 2.0, Roche Diagnostic Systems, Pleasanton, CA), (3) no co-infection with hepatitis B virus or human immunodeficiency virus, (4) no other causes of liver disease, (5) patients having undergone liver biopsy prior to IFN treatment, (6) number of substitutions in ISDR having been determined, (7) substitutions in the amino acid positions 70 and 91 of the core region having been determined, and (8) completion of at least 12 weeks of therapy. Patients were treated with PEG-IFN alpha-2b (1.5 μg/kg) weekly plus RBV. The daily dose of RBV was adjusted by weight: 600 mg for <60 kg, 800 mg for 60–80 kg, and 1,000 mg for >80 kg. For the analysis, patients were assigned randomly to either the model building (304 patients) or validation (201 patients) groups. There were no significant differences in the clinical backgrounds between these two groups (Table I). Informed consent was obtained from each patient. The study protocol conformed to the ethical guidelines of the Declaration of Helsinki and was approved by the institutional review committees of all concerned hospitals.

Laboratory Tests

Hematological tests, blood chemistry, and HCV RNA titer were analyzed before therapy and at least once every month during therapy. Sequences of ISDR and the core region of HCV were determined by direct sequencing after amplification by reverse transcription and polymerase chain reaction as reported previously. At position 70 of the core region (Core70), arginine was defined as the wild type, and glutamine or histidine was defined as the mutant type. At position 91 of the core region, leucine was defined as the wild type and methionine was defined as the mutant type, as described previously [Akuta et al., 2005]. Fibrosis and activity were scored according to the METAVIR scoring system [Bedossa and Poynard, 1996]. Fibrosis was staged on a scale of 0–4: F0 (no fibrosis), F1 (mild fibrosis), F2 (moderate fibrosis), F3 (severe fibrosis), and F4 (cirrhosis). Activity of necroinflammation was graded on a scale of

TABLE I. Comparison of Pretreatment Factors Between Model Building and Validation Patients

	Model (n = 304)	Validation (n = 201)	*P*-value
Age (years)	55.6 (9.4)	56.0 (12.2)	0.80
Male (%)	53 (%)	55 (%)	0.13
Body mass index (kg/m^2)	23.1 (3.1)	23.1 (4.0)	0.99
Albumin (g/dl)	4.0 (0.3)	4.0 (0.3)	0.47
Creatinine (mg/dl)	0.72 (0.15)	0.72 (0.14)	0.62
AST (IU/L)	63.3 (45.6)	58.9 (46.4)	0.91
ALT (IU/L)	78.7 (58.6)	74.5 (67.5)	0.68
GGT (IU/L)	53.2 (49.1)	57.4 (63.5)	0.43
Total cholesterol (mg/dl)	170.9 (32.6)	169.4 (34.1)	0.33
Triglyceride (mg/dl)	107.0 (44.7)	105.7 (48.0)	0.90
LDL-C (mg/dl)	95.5 (28.0)	96.4 (28.8)	0.34
White blood cell count (/μl)	4,902 (1,489)	4,906 (1,319)	0.86
Hemoglobin (g/dl)	14.1 (1.3)	14.3 (1.4)	0.09
Platelets (10^9/L)	164 (56)	172 (55)	0.68
HCVRNA (10^3 IU/ml)	1,859 (1,468)	2,021 (1,393)	0.09
ISDR mutations: ≥2 (%)	15 (%)	20 (%)	0.11
Core70: mutant (%)	36 (%)	29 (%)	0.22
Core91: mutant (%)	40 (%)	36 (%)	0.20
Fibrosis: F2–4 (%)	49 (%)	48 (%)	0.36
Activity: A2–3 (%)	42 (%)	34 (%)	0.10

AST, aspartate aminotransferase; ALT, alanine aminotransferase; GGT, gamma-glutamyltransferase; LDL-C, low-density-lipoprotein-cholesterol; ISDR, interferon sensitivity-determining region.
Data expressed as mean (SD).

0–3: A0 (no activity), A1 (mild activity), A2 (moderate activity), and A3 (severe activity). Sustained virological response was defined as undetectable HCV RNA by qualitative PCR with a lower detection limit of 50 IU/ml (Amplicor, Roche Diagnostic Systems) at week 24 after the completion of therapy.

Statistical Analysis

A database of pretreatment variables included hematological tests (hemoglobin level, white blood cell count, and platelet count), blood chemistry tests (serum levels of creatinine, albumin, aspartate aminotransferase, alanine aminotransferase (ALT), gamma-glutamyltransferase (GGT), total cholesterol, triglyceride, and low-density lipoprotein cholesterol (LDL-C)), viral factors (HCV RNA titer, number of substitutions in ISDR, substitutions in the amino acid positions 70 and 91 of the core region), histological findings (stage of fibrosis and grade of activity) and patient characteristics (age, sex, and body mass index). Based on this database, decision-tree analysis was used to define a predictive model for sustained virological response.

Student's *t*-test was used for the univariable comparison of quantitative variables and Fisher's exact test was used for the comparison of qualitative variables. For the multivariable analysis for factors associated with sustained virological response, logistic regression models with backward selection were used to identify independent predictors of sustained virological response. Variables that showed significant association with sustained virological response by univariable analysis were included in the multivariable analysis. IBM-SPSS software v.15.0 (SPSS, Inc., Chicago, IL) was used for these analyses. For the decision-tree analysis [Segal and Bloch, 1989], the data mining software IBM SPSS Modeler 13 (IBM SPSS, Inc.) was used, as reported previously [Kurosaki et al., 2010a,b]. In brief, the software searched for the optimal split variables to build a decision-tree structure. The entire study population was first evaluated to determine the variables and cut-off points for the most significant division into two subgroups having different probabilities of sustained virological response. Thereafter, analysis was repeated on all subgroups in the same way until either no additional significant variable was detected or the sample size was below 20.

RESULTS

Generation of the Decision-Tree Model

The decision-tree analysis selected five predictive variables to produce six subgroups of patients (Fig. 1). The number of substitutions in ISDR was selected as the best predictor of sustained virological response. The possibility of achieving sustained virological response was 83% for patients with two or more substitutions in ISDR compared with 44% for patients with a single or no substitution. Among patients with a single or no substitution in ISDR, age, with an optimal cut-off of 60 years, was selected as the variable of second split. Patients younger than 60 had the higher probability of sustained virological response (55%) compared with those older than 60 years (31%). Among younger patients, amino acid substitution at Core70 was selected as the third variable of split—wild-type sequence being the predictor of favorable response compared with the mutant type (65% vs. 36%). Among patients with wild-type Core70, the level of serum LDL-C was selected as the fourth variable of split, with an optimal cutoff of

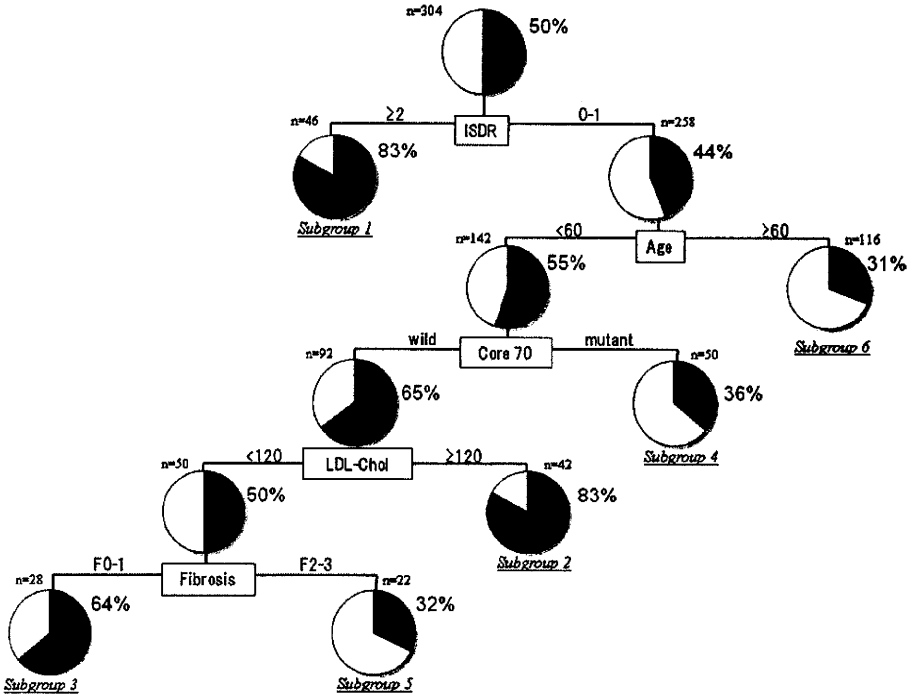

Fig. 1. Decision-tree model. Boxes indicate the factors used for splitting and the cutoff value for the split. Pie charts indicate the rate of sustained virological response for each group of patients after splitting. Terminal subgroups of patients discriminated by the analysis are numbered from 1 to 7. The rate of sustained virological response was >80% in subgroups 1 and 2, 64% in subgroup 3, and 31–36% in subgroups 4, 5, and 6. LDL-C represents low-density lipoprotein cholesterol and Core70 represents amino acid substitution at position 70 of the core region.

120 mg/dl. Patients with higher LDL-C level had the higher probability of sustained virological response (83% vs. 50%). The stage of fibrosis was selected as the final variable of split, with significant fibrosis (F2–4) being the predictor of lower sustained virological response probability (64% vs. 32%).

Among the six subgroups derived by this decision tree, the subgroup of patients with two or more substitutions in ISDR (subgroup 1) or with a single or no substitution in ISDR but younger than 60 years of age, having the wild-type Core70 and high serum level of LDL-C (≥120 mg/dl) (subgroup 2) showed the highest probability of sustained virological response (83%).

Validation of the Decision-Tree Model

The decision-tree model was validated using a validation dataset of 201 cases that were not included the model-building dataset. Each patient in the validation set was allocated to subgroups 1–6 using the flowchart form of the decision tree. The rates of sustained virological response were 75% for subgroup 1, 73% for subgroup 2, 65% for subgroup 3, 41% for subgroup 4, 46% for subgroup 5, and 33% for subgroup 6. The rates of sustained virological response for each subgroup of patients were correlated closely between the model building dataset and the validation dataset ($r^2 = 0.94$) (Fig. 2).

The six subgroups were reconstructed into three groups according to their rate of sustained virological response: the high-probability group consisted of subgroups 1 and 2, the intermediate-probability group consisted of subgroup 3, and the low-probability group consisted of subgroups 4, 5, and 6. The rate of sustained virological response in the high-probability group was high on a consistent basis: 83% for model-building patients and 74% for validation patients. The rate of sustained virological response in the intermediate-probability group was 64% for model building patients and 65% for internal validation patients. The rate of sustained virological response in the low-probability group was low on a consistent basis: 32% for model-building patients and 36% for internal validation patients (Fig. 3). Thirty percent of the patients were classified into the high-probability group and 10% of the patients were classified into intermediate-probability group, which means that about 40% of patients with higher than average probability of achieving sustained virological response were identified.

Effect of Dose Reductions of PEG-IFN and RBV

The possible effect of drug reductions was analyzed in the three groups of patients divided by decision tree (low-, intermediate-, and high-probability groups)

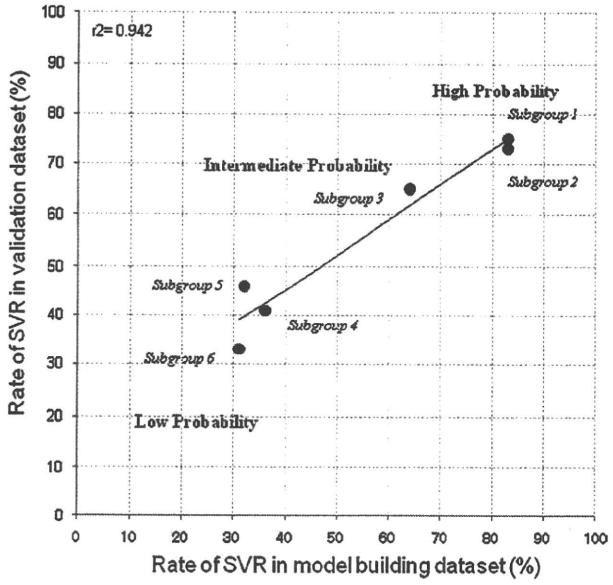

Fig. 2. Validation of the decision-tree analysis: Subgroup-stratified comparison of the rate of sustained virological response. Each patient in the validation set was allocated to subgroups 1–6 by following the flowchart form of the decision tree, and the rates of sustained virological response were then calculated and plotted for each subgroup. The x-axis represents the rate of sustained virological response in the model-building datasets and the y-axis represents the rate of sustained virological response in the validation datasets. The rates of achieving sustained virological response in each subgroup of patients correlated closely between the model-building dataset and the validation dataset (correlation coefficient: $r^2 = 0.94$).

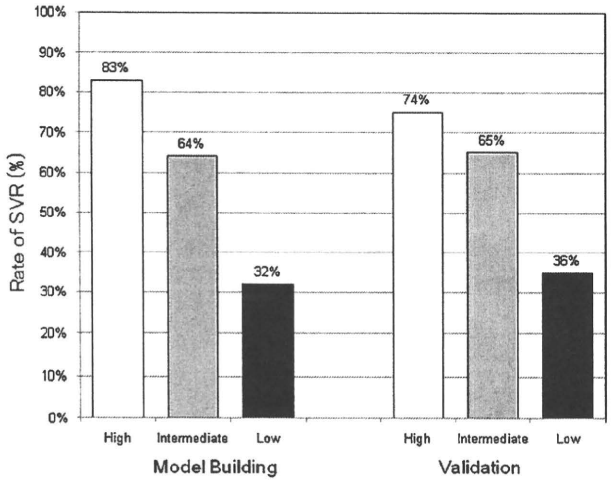

Fig. 3. Comparison of sustained virological response rates between groups divided by the decision tree. The rate of sustained virological response was compared between three groups of patients as divided by the decision-tree analysis. Black, gray, and white boxes indicate the low-probability group (subgroup 4, 5, and 6), intermediate-probability group (subgroup 3), and high-probability group (subgroup 1 and 2), respectively. The rate of sustained virological response showed significant difference between the three groups.

(Fig. 4). Patients were stratified according to the cumulative drug exposure with PEG-IFN and RBV: the good adherence group consisted of patients who took ≥80% planned doses of both PEG-IFN and RBV; the poor adherence group consisted of patients who took <80% of planned doses of both PEG-IFN and RBV. Even after adjustment for drug adherence, the three groups of patients divided by decision-tree analysis still had low, intermediate, and high probability of achieving sustained virological response, respectively, indicating that this model predicts sustained virological response independent of drug exposure.

Multivariable Logistic Regression Analysis

Age, sex, serum levels of creatinine, ALT, GGT, LDL-C, hemoglobin, platelet count, HCV RNA titer, ISDR substitution, substitution at Core70, substitution at Core91, histological stage of fibrosis, and grade of activity were found to be associated with sustained virological response by standard univariable analysis. Multivariable analysis including these factors showed that age, sex, LDL-C levels, GGT levels, platelet count, ISDR substitution, and substitution at Core70 showed independent associations with sustained virological response (Table II). Substitution in ISDR had the highest odds ratio, at 9.92. Fibrosis, which was selected as a significant predictor of response in the decision-tree analysis, was not found to be an independent predictor of response in standard multivariable analysis, indicating that the decision-tree analysis could identify significant predictors that would apply specifically to selected patients.

DISCUSSION

The present study revealed that viral factors such as substitutions in ISDR and Core70 are significant and independent predictors of sustained virological response to PEG-IFN plus RBV in chronic hepatitis C. In a decision-tree model for the pretreatment prediction of sustained virological response, the number of substitutions in ISDR was the best predictor of sustained virological response, followed by younger age, wild-type sequence at Core70, higher level of LDL-C, and absent fibrosis. This decision-tree model could identify patients with high probability of sustained virological response (83%) among difficult-to-treat genotype 1b chronic hepatitis C patients. Using this model, rapid estimates of the response before treatment can be made by allocating patients to specific subgroups with a defined rate of response simply by following the flowchart form. Because more potent therapy, such as a combination of protease inhibitor, PEG-IFN, and RBV, is under clinical trial and may become available in the near future [Hezode et al., 2009; McHutchison et al., 2009], pretreatment prediction of the likelihood of sustained virological response may be useful for both patients and physicians to support clinical decisions whether to start current standard therapy or to wait for emerging new therapies.

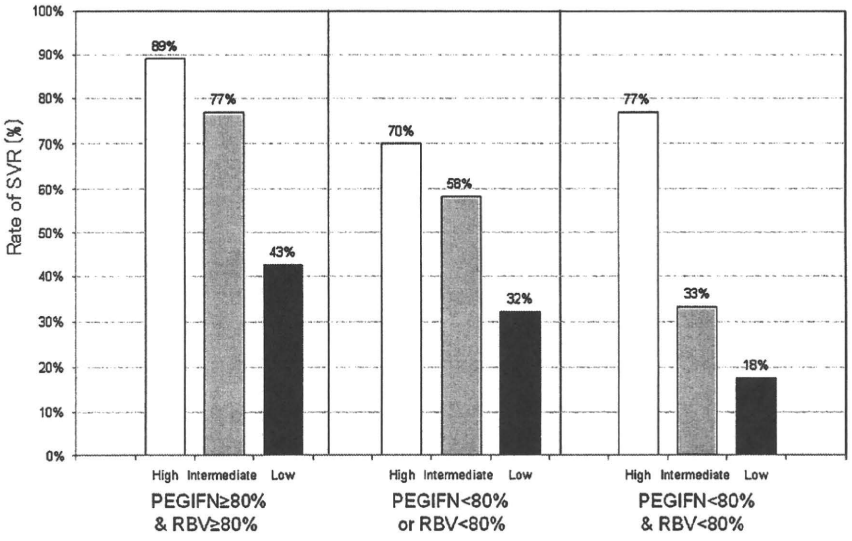

Fig. 4. Comparison of the rate of sustained virological response between the decision-tree groups stratified by drug adherence. The three groups of patients divided by the decision tree (black, gray, and white boxes indicating the low-, intermediate-, and high-probability groups, respectively) were further stratified according to cumulative drug exposure to PEG-IFN and RBV.

Two or more substitutions in ISDR had a strong impact on sustained virological response, because this factor was selected as a top variable in decision-tree analysis and had the highest odds ratio in multivariable analysis. Moreover, even among patients with unfavorable ISDR (0 or 1 mutation), younger patients (<60 years) with the wild-type sequence at Core70 and high level of LDL-C (≥120 mg/dl) had a high rate of sustained virological response. The sustained virological response rate of these two subgroups of patients was 83% in the model-building patients and 75% in the validation patients. Thus, patients with high possibility of sustained virological response could be extracted by the combined analysis of ISDR and Core70. These patients may be the best-suited candidates for treatment with the current combination therapy. Conversely, the following patients with 0–1 mutation in ISDR had a low probability of sustained virological response (32–35%): (1) older (>60 years); or (2) younger (<60 years) patients but having mutant-type sequence at Core70; or (3) younger (<60 years) patients having a wild-type sequence at Core70, but having a low level of LDL-C (<120 mg/dl) and advanced fibrosis. These patients may be advised to wait for a more effective therapy. Decision may be made on a case-by-case basis, taking into account the potential risk of disease progression while waiting.

In a previous decision-tree model using simple and noninvasive standard tests that are available readily worldwide [Kurosaki et al., 2010b], the rate of sustained virological response was at most 65–76% among those in the high-probability group. That model focused on use by general physicians in routine general practice, especially where specialized resources, such as liver biopsy or determination of viral sequences, are not available. In that model, younger age, male sex, higher platelet counts, lower alpha-fetoprotein (AFP) levels, and lower GGT levels were identified as favorable predictive parameters. Higher AFP levels and lower platelet counts that are hallmarks of advanced fibrosis [Shiratori and Omata, 2000; Akuta et al., 2007b] were associated with low probability of sustained virological response in that model. On the other hand, the present analysis aimed to clarify the significance of viral factors for pretreatment prediction of sustained virological response, and to build an advanced model that may be used by specialist physicians engaged in the

TABLE II. Multivariable Logistic Regression Analysis for Factors Associated With SVR

Parameter		Odds	95% CI	*P*-value
Age (years)	<60 vs. ≥60	2.28	1.31–3.94	0.003
Sex	Male vs. female	3.36	1.87–5.99	<0.0001
GGT (IU/L)	<40 vs. ≥40	2.65	1.45–4.85	0.002
LDL-C (mg/dl)	≥120 vs. <120	1.79	0.91–3.53	0.094
Platelets (109/L)	≥120 vs. <120	2.69	1.22–5.90	0.014
ISDR mutations	≥2 vs. 0–1	9.92	3.71–26.54	<0.0001
Core70	Wild vs. mutant	1.92	1.07–3.47	0.030

GGT, gamma-glutamyltransferase; LDL-C, low-density-lipoprotein-cholesterol; ISDR, interferon sensitivity-determining region.

treatment of hepatitis. In the present model, stage of fibrosis was selected as a predictive factor, but at lower level of significance than HCV mutations. The predicted rate of sustained virological response in the high-probability group of the present model is higher than that in the previous model (75–83% vs. 65–76%). These results indicate that substitutions in ISDR and Core70 were important pretreatment predictors of sustained virological response. Determination of these viral factors is not available readily in clinical practice, but is of value for improving the accuracy of pretreatment prediction of sustained virological response.

Substitutions in ISDR and Core70 have been reported previously to be associated with efficacy of IFN therapy. The association between the number of substitutions in ISDR and response to therapy was demonstrated originally in patients treated with IFN mono-therapy [Enomoto et al., 1995, 1996; Kurosaki et al., 1997], but recent studies have reported a positive correlation with PEG-IFN and RBV combination therapy as well [Munoz de Rueda et al., 2008; Shirakawa et al., 2008; Ikeda et al., 2009]. Another important viral factor relevant to treatment response is amino acid substitution in Core70. The sequence of this amino acid was reported originally to be associated with nonresponse to therapy [Akuta et al., 2005], but subsequent studies confirmed the positive correlation of a wild-type Core70 with sustained virological response [Akuta et al., 2009]. The multiple logistic regression analysis showed that ISDR and Core70 were independent factors associated with sustained virological response along with host factors. How these important viral factors and other host factors can be combined to predict response to PEG-IFN plus RBV is an important clinical question. Decision-tree modeling can make the response probability apparent by combining all these factors. Some factors that may be associated with treatment outcome, such as levels of ferritin or homocysteine, were not included. This may be a potential limitation of the present study.

It is of interest that a recent study by Li et al. [2010] has shown that a high serum level of LDL-C is linked to the *IL28B* major allele (CC in rs12979860). In that study, a high serum level of LDL-C was associated with sustained virological response, but it was no longer significant when analyzed together with the *IL28B* genotype in multivariate analysis. Thus, the association between treatment response and LDL cholesterol levels in the present study may reflect the underlining link of LDL cholesterol levels to the *IL28B* genotype. Recent reports indicate that the *IL28B* genotype and HCV substitutions are correlated closely [Akuta et al., 2010; Kurosaki et al., 2010c]. Still, Core70 [Akuta et al., 2010] or ISDR [Kurosaki et al., 2010c] were predictors of response to therapy independent of *IL28B* genotype. Future study is needed to elucidate the possible mechanisms underlying the association between HCV sequences and host genetic factors, and also the role of host and viral factors for the prediction of treatment response.

In conclusion, a data mining analysis emphasized the impact of substitutions in ISDR and Core70 on pretreatment prediction of sustained virological response to PEG-IFN plus RBV therapy. A decision-tree model that includes substitutions in ISDR and Core70 of HCV could identify patients with high probability of sustained virological response, and could thereby improve the predictive accuracy over predictions that are based on standard tests.

REFERENCES

Akuta N, Suzuki F, Sezaki H, Suzuki Y, Hosaka T, Someya T, Kobayashi M, Saitoh S, Watahiki S, Sato J, Matsuda M, Arase Y, Ikeda K, Kumada H. 2005. Association of amino acid substitution pattern in core protein of hepatitis C virus genotype 1b high viral load and non-virological response to interferon-ribavirin combination therapy. Intervirology 48:372–380.

Akuta N, Suzuki F, Kawamura Y, Yatsuji H, Sezaki H, Suzuki Y, Hosaka T, Kobayashi M, Arase Y, Ikeda K, Kumada H. 2007a. Predictive factors of early and sustained responses to peginterferon plus ribavirin combination therapy in Japanese patients infected with hepatitis C virus genotype 1b: Amino acid substitutions in the core region and low-density lipoprotein cholesterol levels. J Hepatol 46:403–410.

Akuta N, Suzuki F, Kawamura Y, Yatsuji H, Sezaki H, Suzuki Y, Hosaka T, Kobayashi M, Arase Y, Ikeda K, Kumada H. 2007b. Predictors of viral kinetics to peginterferon plus ribavirin combination therapy in Japanese patients infected with hepatitis C virus genotype 1b. J Med Virol 79:1686–1695.

Akuta N, Suzuki F, Hirakawa M, Kawamura Y, Yatsuji H, Sezaki H, Suzuki Y, Hosaka T, Kobayashi M, Saitoh S, Arase Y, Ikeda K, Kumada H. 2009. A matched case-controlled study of 48 and 72 weeks of peginterferon plus ribavirin combination therapy in patients infected with HCV genotype 1b in Japan: Amino acid substitutions in HCV core region as predictor of sustained virological response. J Med Virol 81:452–458.

Akuta N, Suzuki F, Hirakawa M, Kawamura Y, Yatsuji H, Sezaki H, Suzuki Y, Hosaka T, Kobayashi M, Saitoh S, Arase Y, Ikeda K, Chayama K, Nakamura Y, Kumada H. 2010. Amino acid substitution in hepatitis C virus core region and genetic variation near the interleukin 28B gene predict viral response to telaprevir with peginterferon and ribavirin. Hepatology 52:421–429.

Averbook BJ, Fu P, Rao JS, Mansour EG. 2002. A long-term analysis of 1018 patients with melanoma by classic Cox regression and tree-structured survival analysis at a major referral center: Implications on the future of cancer staging. Surgery 132:589–602.

Baquerizo A, Anselmo D, Shackleton C, Chen TW, Cao C, Weaver M, Gornbein J, Geevarghese S, Nissen N, Farmer D, Demetriou A, Busuttil RW. 2003. Phosphorus ans an early predictive factor in patients with acute liver failure. Transplantation 75:2007–2014.

Bedossa P, Poynard T. 1996. An algorithm for the grading of activity in chronic hepatitis C. The METAVIR Cooperative Study Group. Hepatology 24:289–293.

Breiman LJH, Friedman RA, Olshen CJ, Stone CM. 1980. Classification and regression trees. CA: Wadsworth.

Davis GL, Wong JB, McHutchison JG, Manns MP, Harvey J, Albrecht J. 2003. Early virologic response to treatment with peginterferon alfa-2b plus ribavirin in patients with chronic hepatitis C. Hepatology 38:645–652.

Enomoto N, Sakuma I, Asahina Y, Kurosaki M, Murakami T, Yamamoto C, Izumi N, Marumo F, Sato C. 1995. Comparison of full-length sequences of interferon-sensitive and resistant hepatitis C virus 1b. Sensitivity to interferon is conferred by amino acid substitutions in the NS5A region. J Clin Invest 96:224–230.

Enomoto N, Sakuma I, Asahina Y, Kurosaki M, Murakami T, Yamamoto C, Ogura Y, Izumi N, Marumo F, Sato C. 1996. Mutations in the nonstructural protein 5A gene and response to interferon in patients with chronic hepatitis C virus 1b infection. N Engl J Med 334:77–81.

Fried MW, Shiffman ML, Reddy KR, Smith C, Marinos G, Goncales FL, , Haussinger D, Diago M, Carosi G, Dhumeaux D, Craxi A, Lin A, Hoffman J, Yu J. 2002. Peginterferon alfa-2a plus ribavirin for chronic hepatitis C virus infection. N Engl J Med 347:975–982.

Garzotto M, Beer TM, Hudson RG, Peters L, Hsieh YC, Barrera E, Klein T, Mori M. 2005. Improved detection of prostate cancer using classification and regression tree analysis. J Clin Oncol 23:4322–4329.

Ge D, Fellay J, Thompson AJ, Simon JS, Shianna KV, Urban TJ, Heinzen EL, Qiu P, Bertelsen AH, Muir AJ, Sulkowski M, McHutchison JG, Goldstein DB. 2009. Genetic variation in IL28B predicts hepatitis C treatment-induced viral clearance. Nature 461:399–401.

Hezode C, Forestier N, Dusheiko G, Ferenci P, Pol S, Goeser T, Bronowicki JP, Bourliere M, Gharakhanian S, Bengtsson L, McNair L, George S, Kieffer T, Kwong A, Kauffman RS, Alam J, Pawlotsky JM, Zeuzem S. 2009. Telaprevir and peginterferon with or without ribavirin for chronic HCV infection. N Engl J Med 360: 1839–1850.

Ikeda H, Suzuki M, Okuse C, Yamada N, Okamoto M, Kobayashi M, Nagase Y, Takahashi H, Matsunaga K, Matsumoto N, Itoh F, Yotsuyanagi H, Koitabashi Y, Yasuda K, Iino S. 2009. Short-term prolongation of pegylated interferon and ribavirin therapy for genotype 1b chronic hepatitis C patients with early viral response. Hepatol Res 39:753–759.

Izumi N, Nishiguchi S, Hino K, Suzuki F, Kumada Y, Itoh Y, Asahina Y, Tamori A, Hiramatsu N, Hayashi N, Kudo M. 2010. Management of hepatitis C; Report of the consensus meeting at the 45th annual meeting of the Japan society of hepatology (2009). Hepatol Res 40:347–368.

Jensen DM, Morgan TR, Marcellin P, Pockros PJ, Reddy KR, Hadziyannis SJ, Ferenci P, Ackrill AM, Willems B. 2006. Early identification of HCV genotype 1 patients responding to 24 weeks peginterferon alpha-2a (40 kd)/ribavirin therapy. Hepatology 43:954–960.

Kurosaki M, Enomoto N, Murakami T, Sakuma I, Asahina Y, Yamamoto C, Ikeda T, Tozuka S, Izumi N, Marumo F, Sato C, Ogura Y. 1997. Analysis of genotypes and amino acid residues 2209 to 2248 of the NS5A region of hepatitis C virus in relation to the response to interferon-beta therapy. Hepatology 25:750–753.

Kurosaki M, Matsunaga K, Hirayama I, Tanaka T, Sato M, Yasui Y, Tamaki N, Hosokawa T, Ueda K, Tsuchiya K, Nakanishi H, Ikeda H, Itakura J, Takahashi Y, Asahina Y, Higak M, Enomoto N, Izumi N. 2010a. A predictive model of response to peginterferon ribavirin in chronic hepatitis C using classification and regression tree analysis. Hepatol Res 40:251–260.

Kurosaki M, Sakamoto N, Iwasaki M, Sakamoto M, Suzuki Y, Hiramatsu N, Sugauchi F, Yatsuhashi H, Izumi N. 2010b. Pretreatment prediction of response to peginterferon plus ribavirin therapy in genotype 1 chronic hepatitis C using data mining analysis. J Gastroenterol DOI: 10.1007/s00535-010-0322-5.

Kurosaki M, Tanaka Y, Nishida N, Sakamoto N, Enomoto N, Honda M, Sugiyama M, Matsuura K, Sugauchi F, Asahina Y, Nakagawa M, Watanabe M, Sakamoto M, Maekawa S, Sakai A, Kaneko S, Ito K, Masaki N, Tokunaga K, Izumi N, Mizokami M. 2010c. Pretreatment prediction of response to pegylated-interferon plus ribavirin for chronic hepatitis C using genetic polymorphism in *IL28B* and viral factors. J Hepatol DOI: 10.1016/j.jhep.2010.07.037.

LeBlanc M, Crowley J. 1995. A review of tree-based prognostic models. Cancer Treat Res 75:113–124.

Lee SS, Ferenci P. 2008. Optimizing outcomes in patients with hepatitis C virus genotype 1 or 4. Antivir Ther 13:9–16.

Leiter U, Buettner PG, Eigentler TK, Garbe C. 2004. Prognostic factors of thin cutaneous melanoma: An analysis of the central malignant melanoma registry of the German Dermatological Society. J Clin Oncol 22:3660–3667.

Li JH, Lao XQ, Tillmann HL, Rowell J, Patel K, Thompson A, Suchindran S, Muir AJ, Guyton JR, Gardner SD, McHutchison JG, McCarthy JJ. 2010. Interferon-lambda genotype and low serum low-density lipoprotein cholesterol levels in patients with chronic hepatitis C infection. Hepatology 51:1904–1911.

Manns MP, McHutchison JG, Gordon SC, Rustgi VK, Shiffman M, Reindollar R, Goodman ZD, Koury K, Ling M, Albrecht JK. 2001. Peginterferon alfa-2b plus ribavirin compared with interferon alfa-2b plus ribavirin for initial treatment of chronic hepatitis C: A randomised trial. Lancet 358:958–965.

McHutchison JG, Everson GT, Gordon SC, Jacobson IM, Sulkowski M, Kauffman R, McNair L, Alam J, Muir AJ. 2009. Telaprevir with peginterferon and ribavirin for chronic HCV genotype 1 infection. N Engl J Med 360:1827–1838.

Miyaki K, Takei I, Watanabe K, Nakashima H, Omae K. 2002. Novel statistical classification model of type 2 diabetes mellitus patients for tailor-made prevention using data mining algorithm. J Epidemiol 12:243–248.

Munoz de Rueda P, Casado J, Paton R, Quintero D, Palacios A, Gila A, Quiles R, Leon J, Ruiz-Extremera A, Salmeron J. 2008. Mutations in E2-PePHD, NS5A-PKRBD, NS5A-ISDR, and NS5A-V3 of hepatitis C virus genotype 1 and their relationships to pegylated interferon-ribavirin treatment responses. J Virol 82:6644–6653.

Segal MR, Bloch DA. 1989. A comparison of estimated proportional hazards models and regression trees. Stat Med 8:539–550.

Shirakawa H, Matsumoto A, Joshita S, Komatsu M, Tanaka N, Umemura T, Ichijo T, Yoshizawa K, Kiyosawa K, Tanaka E. 2008. Pretreatment prediction of virological response to peginterferon plus ribavirin therapy in chronic hepatitis C patients using viral and host factors. Hepatology 48:1753–1760.

Shiratori Y, Omata M. 2000. Predictors of the efficacy of interferon therapy for patients with chronic hepatitis C before and during therapy: How does this modify the treatment course? J Gastroenterol Hepatol 15:E141–E151.

Suppiah V, Moldovan M, Ahlenstiel G, Berg T, Weltman M, Abate ML, Bassendine M, Spengler U, Dore GJ, Powell E, Riordan S, Sheridan D, Smedile A, Fragomeli V, Muller T, Bahlo M, Stewart GJ, Booth DR, George J. 2009. IL28B is associated with response to chronic hepatitis C interferon-alpha and ribavirin therapy. Nat Genet 41:1100–1104.

Tanaka Y, Nishida N, Sugiyama M, Kurosaki M, Matsuura K, Sakamoto N, Nakagawa M, Korenaga M, Hino K, Hige S, Ito Y, Mita E, Tanaka E, Mochida S, Murawaki Y, Honda M, Sakai A, Hiasa Y, Nishiguchi S, Koike A, Sakaida I, Imamura M, Ito K, Yano K, Masaki N, Sugauchi F, Izumi N, Tokunaga K, Mizokami M. 2009. Genome-wide association of IL28B with response to pegylated interferon-alpha and ribavirin therapy for chronic hepatitis C. Nat Genet 41:1105–1109.

Valera VA, Walter BA, Yokoyama N, Koyama Y, Iiai T, Okamoto H, Hatakeyama K. 2007. Prognostic groups in colorectal carcinoma patients based on tumor cell proliferation and classification and regression tree (CART) survival analysis. Ann Surg Oncol 14:34–40.

Yu ML, Dai CY, Huang JF, Chiu CF, Yang YH, Hou NJ, Lee LP, Hsieh MY, Lin ZY, Chen SC, Wang LY, Chang WY, Chuang WL. 2008. Rapid virological response and treatment duration for chronic hepatitis C genotype 1 patients: A randomized trial. Hepatology 47:1884–1893.

Zlobec I, Steele R, Nigam N, Compton CC. 2005. A predictive model of rectal tumor response to preoperative radiotherapy using classification and regression tree methods. Clin Cancer Res 11:5440–5443.

J Gastroenterol (2011) 46:350–358
DOI 10.1007/s00535-010-0301-x

ORIGINAL ARTICLE—LIVER, PANCREAS, AND BILIARY TRACT

Real-time tissue elastography as a tool for the noninvasive assessment of liver stiffness in patients with chronic hepatitis C

Hiroyasu Morikawa · Katsuhiko Fukuda · Sawako Kobayashi · Hideki Fujii · Shuji Iwai · Masaru Enomoto · Akihiro Tamori · Hiroki Sakaguchi · Norifumi Kawada

Received: 6 May 2010 / Accepted: 15 July 2010 / Published online: 10 August 2010

Abstract
Background Although histopathological examination by "invasive" liver biopsy remains the gold standard for evaluating disease progression in chronic liver disease, noninvasive tools have appeared and have led to great progress in diagnosing the stage of hepatic fibrosis. The aim of this study was to assess the value of real-time tissue elastography, using an instrument made in Japan, for the visible measurement of liver elasticity; in particular, comparing the results with those of transient elastography (Fibroscan).
Methods Real-time tissue elastography (RTE), transient elastography (Fibroscan), liver biopsy, and routine laboratory analyses were performed in 101 patients with chronic hepatitis C. The values for tissue elasticity obtained using novel software (Elasto_ver 1.5.1) connected to RTE were transferred to four image features, Mean, Standard Deviation (SD), Area, and Complexity. Their association with the stage of fibrosis at biopsy and with liver stiffness (kPa) obtained by Fibroscan was analyzed.
Results Colored images obtained by RTE were classified into diffuse soft, intermediate, and patchy hard patterns and the calculated elasticity differed significantly between patients according to and correlated with the stages of fibrosis ($p < 0.0001$). Mean, SD, Area, and Complexity showed significant differences between the stages of fibrosis (Tukey–Kramer test, $p < 0.05$). In discriminating patients with cirrhosis, the areas under the receiver operating characteristic curves (AUC) were 0.91 for Mean, 0.84 for SD, 0.91 for Area, 0.93 for Complexity, and 0.95 for Fibroscan.
Conclusions RTE is a noninvasive instrument for the colored visualization of liver elasticity in patients with chronic liver disease.

Keywords Liver fibrosis · Transient elastography · Ultrasound · Liver biopsy

H. Morikawa · S. Kobayashi · H. Fujii · S. Iwai · M. Enomoto · A. Tamori · H. Sakaguchi · N. Kawada (✉)
Department of Hepatology, Graduate School of Medicine, Osaka City University, 1-4-3 Asahimachi, Abeno, Osaka 545-8585, Japan
e-mail: kawadanori@med.osaka-cu.ac.jp

K. Fukuda
Department of Gastroenterology, PL Hospital, Tondabayashi, Japan

Introduction

Hepatitis C virus (HCV) infects approximately 170 million individuals worldwide, according to a report from the World Health Organization [1]. Chronic liver damage attributable to HCV infection results in hepatic fibrosis, which is characterized by an unusual accumulation of extracellular matrix materials produced by fibroblast-like cells including stellate cells in the hepatic parenchyma. Hepatic fibrosis progresses towards cirrhosis, an end-stage liver injury, leading to hepatic failure, hepatocellular carcinoma, and finally death. Thus, precise evaluation of the stage of chronic hepatitis C with respect to fibrosis has become an important issue to prevent the occurrence of cirrhosis and to initiate appropriate therapeutic intervention such as viral eradication using pegylated interferon (PEG-IFN) plus ribavirin [2].

Although liver biopsy is acknowledged as the gold standard for staging disease progression, there are some limitations, including its invasiveness, risk of complications, sampling error, variability in histopathological interpretation, and the reluctance of patients to submit to repeated examinations [3]. Because of these disadvantages, there is a

growing shift in clinical practice to utilize or develop 'non-invasive' methodologies to reflect the stage of liver fibrosis.

Several noninvasive approaches have appeared, such as serum fibrosis markers, transient elastography (Fibroscan®; Echosens SA, Paris, France), and real-time tissue elastography (RTE). Serum fibrosis markers include direct tests, such as hyaluronic acid and type IV collagen, and indirect approaches, which detect alterations in hepatic function but do not directly reflect hepatic extracellular matrix metabolism; these include platelet counts, coagulation studies, and hepatic transaminases, or their combinations in indices/scores, such as the aspartate aminotransferase-to-platelet ratio index (APRI) [4, 5].

Transient elastography, which has been developed for the measurement of liver stiffness, is considered to reflect more directly than other means the fibrotic evolution of chronic liver trauma [6–10]. In 2005, Castera et al. and Ziol et al. reported that liver stiffness measurements could be useful in assessing the presence of significant fibrosis (F2–4) and in suggesting the presence of cirrhosis in cohorts of patients with chronic hepatitis C; the areas under the receiver operating characteristic curves (AUCs) ranged from 0.79 to 0.83 for the prediction of F2–4 and were over 0.95 for the identification of cirrhosis [11, 12]. Friedrich-Rust et al. [13] assessed the overall performance of transient elastography for the diagnosis of liver fibrosis by a meta-analysis which included fifty articles; the mean AUCs for the diagnosis of significant fibrosis, severe fibrosis, and cirrhosis were 0.84, 0.89, and 0.94, respectively. The limitations of this method have also been discussed; intraobserver agreement is influenced by variables such as body mass index (BMI, particularly when $\geq$28), hepatic steatosis, and flares of transaminases [11–14].

RTE is a method developed in Japan for the visual assessment of tissue elasticity integrated in a sonography machine, based on a Combined Autocorrelation Method that calculates the relative hardness of tissue rapidly from the degree of tissue distortion and which displays this information as a color image. The distortion of tissue is color-coded according to its magnitude and superimposed translucently on a conventional B-mode image. This simultaneous display enables us to evaluate the anatomical correspondence between tissue elasticity and B-mode images. The RTE image is constructed by the amount of displacement of the reflected ultrasound echoes under compression. Ultrasound elastography does not demonstrate physical elasticity directly, but shows the relative degree of tissue strain when subtle compression is applied. In hard tissue, the amount of displacement of the reflected ultrasound echoes is low, whereas in soft tissue, the amount of displacement is higher because soft tissue can be compressed more than hard tissue [15, 16]. This technology has already been proved to be diagnostically valuable in detecting space-occupying lesions in the breast, prostate, and pancreas [17–20]. Friedrich-Rust et al. [21] attempted to determine the elasticity of liver tissue in 79 patients with chronic viral hepatitis. They developed an elasticity score from the color-coded bit-map image produced by the computer program Mathlab version 6 (Math Works, Natick, MA, US). However, the diagnostic accuracy of this semi-quantitative assessment for the prediction of significant fibrosis (METAVIR scoring system $\geq$F2), severe fibrosis ($\geq$F3), and cirrhosis (F4) was not satisfactory; the AUCs were 0.75, 0.73, and 0.69, respectively [21].

We report here an updated RTE system as a tool for the noninvasive assessment of liver stiffness in patients with chronic hepatitis C. In this new system, all pixel data in the colored image were transformed into a histogram and a binary image for more accurate quantification, using an exclusive software program.

Methods

Patients

Ten healthy adult volunteers with no evident liver disease were recruited after giving their oral informed consent. One hundred and one patients with chronic hepatitis C, whose disease was defined by the presence of serum anti-hepatitis C virus (HCV) antibodies and serum HCV RNA, with serum levels of alanine aminotransferase above the upper limit of normal, were included in this study. Percutaneous liver biopsy or laparoscopy was performed on the patients within 1 week following Fibroscan and RTE analysis at the Department of Hepatology, Osaka City University Hospital, between September 2007 and September 2009. The study protocol accorded with the Helsinki Declaration and was approved by the ethics committee of our institution. Patients were enrolled and liver biopsy was performed after informed consent was obtained.

Liver histology and quantification of liver fibrosis

Liver biopsy was carried out using a 15-gauge Tru-Cut needle biopsy apparatus (Hakko, Tokyo, Japan). The median length of liver samples obtained at biopsy was 18 mm (range 10–25 mm). Tissue specimens obtained by liver biopsy were fixed immediately in 10% formalin solution and embedded in paraffin. After cutting, sections were stained with hematoxylin and eosin or Azan Mallory and the stage of fibrosis and grade of inflammatory activity in the liver were determined according to the METAVIR scoring system [22, 23]. All biopsy specimens were examined independently by two experienced pathologists who were blinded to the clinical data and the measurements

of liver stiffness. Fibrosis was staged on a 0–4 scale as follows: F0, no fibrosis; F1, portal fibrosis without septa; F2, portal fibrosis and few septa; F3, numerous septa without cirrhosis; F4, cirrhosis. The chronic hepatitis activity was graded as follows: A0, none; A1, mild; A2, moderate; and A3, severe.

Real-time elastography

We used ultrasonography (Hitachi EUB-8500; Hitachi Medical, Chiba, Japan) and an EUP-L52 Linear probe (3–7 MHz; Hitachi Medical) for real-time tissue elastography (RTE). This system is commercially available currently for the diagnosis of mammary neoplasms [17].

Patients were examined in a supine position with the right arm elevated above the head, and were instructed to hold their breath. The examination was performed on the right lobe of the liver through the intercostals, because liver biopsy and Fibroscan were also performed at the same site. The RTE equipment displays two images simultaneously; the RTE image showing the region of interest (ROI) as a colored area and the conventional B-mode image (Fig. 1a). An area was chosen where the tissue was free of large vessels and near the biopsy point. The measurement was fixed to a rectangle with 30 mm length × 20 mm breadth placed 5 mm below the surface of the liver (Fig. 1a). The color in the ROI was graded from blue to red (Fig. 1b). We stored the RTE images as moving digital images for 20–40 s. Then ten static images, captured by the observer at random from the moving images, using AVI2JPG v6.10 converter software (Novo, Tokyo, Japan), were analyzed using the novel software Elasto_ver 1.5.1 (which was developed and donated by Hitachi Medical) on a personal computer. Numerical values of pixels were from 0 to 255 (256 stepwise grading) according to color mapping from blue (0) to red (255), and a histogram of the distribution was generated (Fig. 1c). The scale ranged from red for components with the greatest strain (i.e., softest components) to blue for those with no strain (i.e., hardest components). Green indicated average strain in the ROI, and therefore intact liver tissue displayed a diffuse homogeneous green pattern. An appearance of unevenness in the color pattern was considered to reflect a change in the liver stiffness. For quantification, all pixel data in the colored image were transformed into a histogram and binary image (Fig. 1c, d).

Colored RTE images are usually classified into several patterns in the diagnosis of breast disease [17]. In this study, we evaluated liver fibrosis as three patterns: a diffuse soft pattern, an intermediate pattern, and a patchy hard pattern. The diffuse soft pattern was a relatively homogeneously spread, light-green colored image (Fig. 2a; the corresponding histology is shown in Fig. 2d). The intermediate pattern was typified by a partially mottled, dotted image with blue spots on a light green background (Fig. 2b; the corresponding histology is shown in Fig. 2e). The patchy hard pattern comprised mixed images with a patchwork effect of light green, red, and blue (Fig. 2c; the corresponding histology is shown in Fig. 2f).

Transient elastography

Liver stiffness was also measured by transient elastography (Fibroscan®; Echosens SA, Paris, France). Briefly, patients were placed on the bed in the horizontally supine position. A probe was placed on the skin above the right intercostal space. The velocity of shear waves, which were generated temporarily and passed though the liver, was combined with Young's modulus for the automated calculation of elasticity [9]. Ten successful acquisitions were performed on each patient. The results that obtained ten valid measurements with a success rate of at least 60% and an interquartile range under 30% were considered successful. A median of 10 valid measurements was regarded as the liver stiffness for a given subject, and expressed in kilopascals (kPa).

APRI

The APRI was calculated as follows: aspartate aminotransferase (/upper limit of normal) × 10/platelet count (10^4/mm^3).

Statistical analysis

Box plots were used to study the distribution of the RTE values according to the stage of fibrosis. The trends were evaluated using the Jonckheere–Terpstra test. The Tukey–Kramer test was used to compare the data between the groups. The diagnostic performance of RTE parameters and transient elastography was assessed with receiver operating characteristic (ROC) curves. The ROC curve is a plot of the sensitivity versus 1-specificity for all possible cutoff values. The most commonly used index of accuracy is the area under the receiving operating characteristic curve (AUC), with values close to 1.0 indicating high diagnostic accuracy. Analyses were performed using JMP-8 software (SAS Institute, Cary, USA).

Results

Patients

The characteristics of our 101 patients with chronic HCV infection at the time of RTE and transient elastography are summarized in Table 1. In 91 of them, liver biopsy was performed successfully. Ten patients, who had no clinically

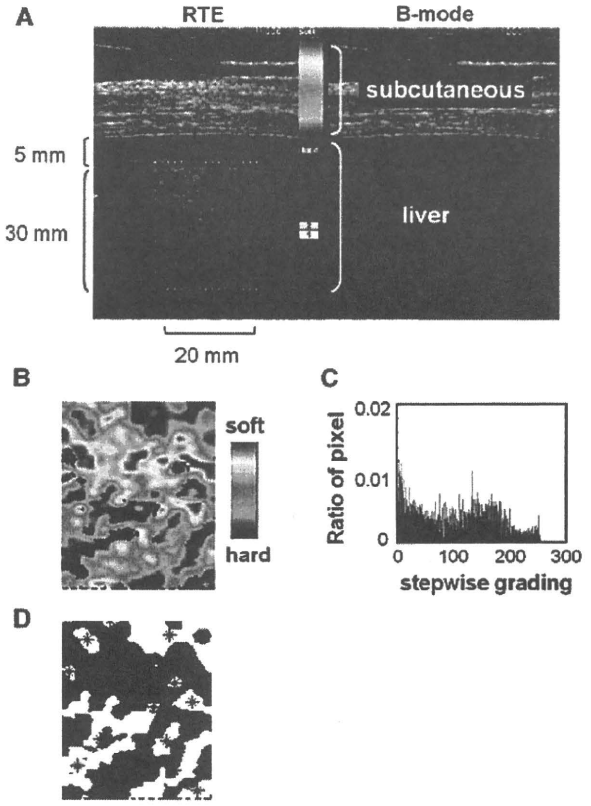

Fig. 1 Procedure of image analyses for real-time tissue elastography (*RTE*). **a** The region of interest (ROI) was fixed to a rectangle with about 30 mm length × about 20 mm breadth with a 400–600 mm^2 area placed 5 mm below the surface of the liver. **b** The color-coded images from the ROI of RTE were analyzed by the software Elasto_ver 1.5.1. The colors ranged from *blue to red,* indicating the relative gradients from hardness to softness. **c** Mean and Standard Deviation were calculated by a histogram, which was generated by 256 stepwise grading derived from the color image obtained in **b**. **d** Area and Complexity were calculated from the binary image. Area was derived from the percentage of *white regions* (*asterisks*, i.e., hard area). Complexity was calculated by the following equation, $periphery^2/Area$. Median value of the data was kept as representative of RTE parameters

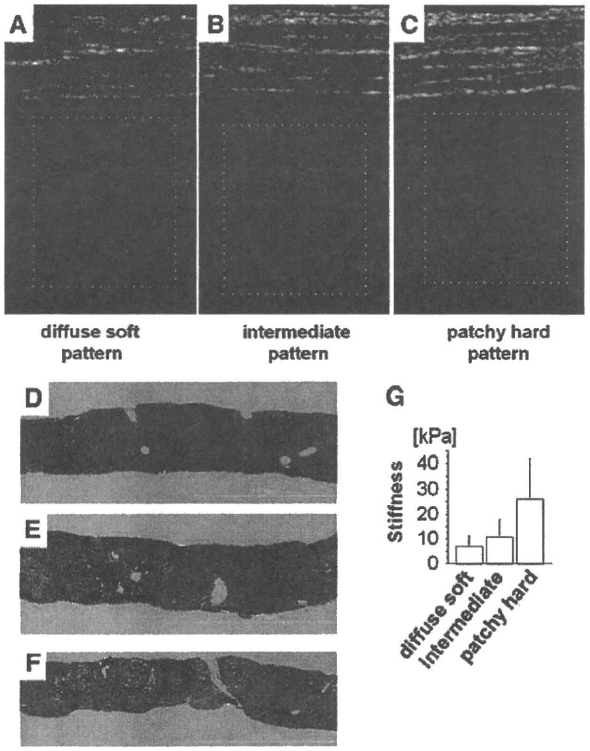

Fig. 2 Representative colored images of real-time tissue elastography. **a** A case of F1 whose histology is shown in **d**. Relatively homogeneous image colored *light green* indicates a diffuse soft pattern in RTE. Liver stiffness measured by transient elastography (Fibroscan) was 4.1 kPa. **b** A case of F3 whose histology is shown in **e**. Partially mottled and dotted image with blue and red spots in the light green background indicates an intermediate pattern in RTE. Liver stiffness measured by Fibroscan was 9.6 kPa. **c** A case of F4 whose histology is shown in **f**. Mixed image with *light green*, *blue*, and *red colors* indicates patchy hard pattern. Liver stiffness measured by Fibroscan was 36.3 kPa. **g** Correlation of the averages of liver stiffness measured by Fibroscan with the three patterns of RTE images. The transition of these three patterns correlated positively with the liver stiffness ($p < 0.01$). **d–f** H&E staining. *Yellow bars* 2 mm

overt sign of decompensated cirrhosis, were diagnosed with cirrhosis (F4) by the appearance of the liver surface at laparoscopy without liver biopsy. RTE was performed successfully in all patients, but five patients (F1, 2; F3, 1; F4, 2) failed to receive transient elastography measurements due to obesity and liver atrophy.

Representative images of real-time tissue elastography

The results were described as the Mean, which indicates the mean of the histogram and ranges from 73.0 to 139.8 (median 111.9), and Standard Deviation (SD), which indicates the standard deviation of the histogram and ranges from 36.5 to 76.6 (median 60.8). In another analysis, the data were transformed into a binary image and the results were described as Area, which indicates the percentage of hard tissue and represents the hard tissue domain divided by the ROI and ranges from 5.0 to 54.7% (median 24.8%), and Complexity, which indicates the complex ratio of the shape of an extracted hard tissue domain in the ROI and is calculated as $periphery^2$/area of the hard tissue domain and ranges from 15.9 to 40.21 (median 22.9) (Fig. 1d). The four image features were calculated automatically by Elasto_ver 1.5.1 (Hitachi Medical). Mean, SD, and Complexity were described in arbitrary units [a.u.].

The colored RTE images were classified into three patterns according to their visual appearance. The values for liver stiffness measurement by transient elastography (Fibroscan) were 6.9 ± 4.5, 10.9 ± 6.8, and 26.0 ± 15.8 kPa in the diffuse soft pattern group, intermediate pattern group, and patchy

Table 1 Characteristics of the patients at the time of real-time tissue elastography examination

Characteristics	Patients ($n = 101$)
Sex: male/female	43/58
Age (years)	54 ± 13 (range 24–80)
BMI (kg/m^2)	22.1 ± 3.1 (range 15.1–32.3)
Platelet count ($\times 10^4$/mm^3)	16.4 ± 6.6
Total bilirubin (mg/dL)	0.9 ± 0.4
Prothrombin time (INR)	1.02 ± 0.1
ALT (IU/L)	58.2 ± 41.2
Fibrosis stage	
F0	6
F1	48
F2	15
F3	16
F4	16
Histological activity of 91 patients with liver biopsy	
A0	2
A1	24
A2	45
A3	20

Values are means ± SEM

BMI body mass index, *ALT* alanine aminotransferase

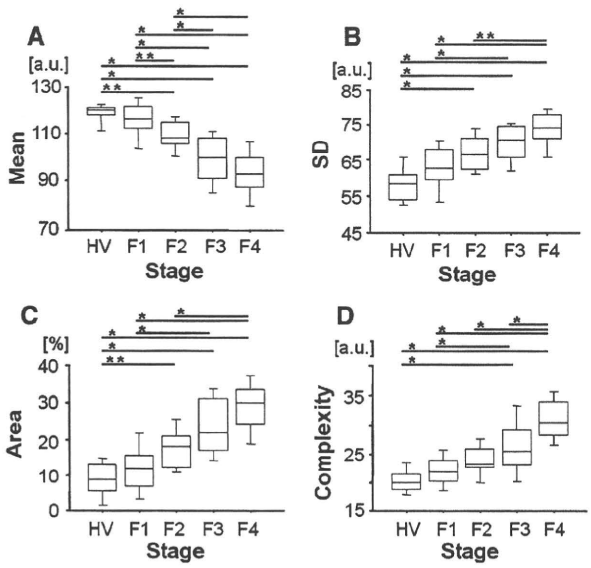

Fig. 3 Parameter analyses measured by real-time tissue elastography (RTE) for each fibrosis stage. Box plots of each RTE value corresponding to fibrosis stages F1–4 and the healthy volunteer group (*HV*). The *tops and bottoms of the boxes* indicate the 1st and 3rd quartiles. The *length of the box* represents the interquartile range within which 50% of values are located. The *lines through the middles of the boxes* represent the medians. **a** Mean, **b** SD, **c** Area, and **d** Complexity. HV, $n = 10$. F1–4, $n = 95$. $*p < 0.01$, and $**p < 0.05$

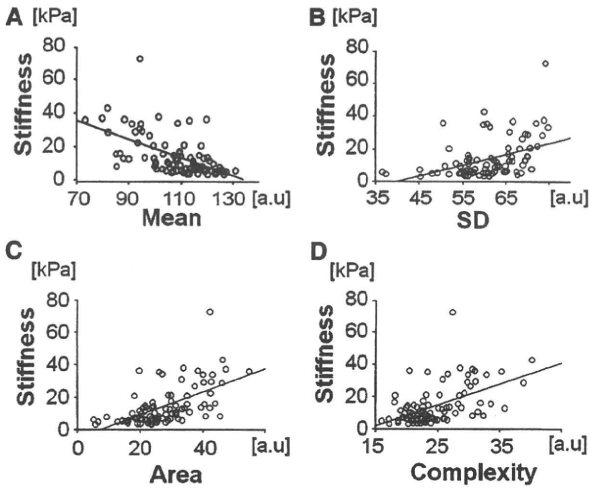

Fig. 4 Correlation between liver stiffness measured by transient elastography (Fibroscan) and the parameters of real-time tissue elastography. **a** Mean was negatively correlated with liver stiffness (kPa) ($p < 0.01$). Correlation coefficient was −0.585. **b** SD was significantly correlated with liver stiffness (kPa) ($p < 0.01$). Correlation coefficient was 0.425. **c** Area was significantly correlated with liver stiffness (kPa) ($p < 0.01$). Correlation coefficient was 0.590. **d** Complexity was significantly correlated with liver stiffness (kPa) ($p < 0.01$). Correlation coefficient was 0.532 ($n = 96$). *a.u.* arbitrary units

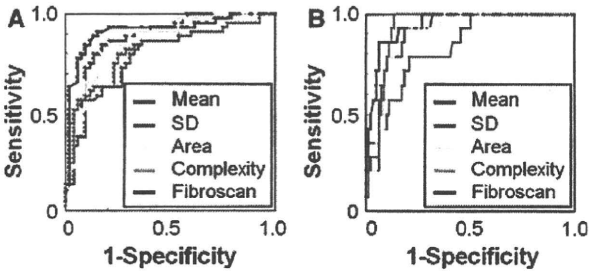

Fig. 5 Receiver operating characteristic curves of each parameter obtained by RTE. **a** No significant fibrosis (F0–1). **b** Cirrhosis (F4). **a** The areas under the receiver operating characteristic curves (AUC) for no significant fibrosis (F0–1) were 0.89, 0.81, 0.87, 0.81, and 0.92 for Mean (*red*), SD (*blue*), Area (*yellow*), Complexity (*pink*), and transient elastography (Fibroscan, *black*), respectively. **b** The AUCs for cirrhosis were 0.91, 0.84, 0.91, 0.93, and 0.95 for Mean, SD, Area, and Complexity, and transient elastography, respectively ($n = 96$)

hard pattern group, respectively. Thus, these three patterns correlated significantly with the kPa values obtained by transient elastography (Jonckheere–Terpstra test, $p < 0.0001$) (Fig. 2g).

Relationship between real-time tissue elastography and histological parameters

Figure 3a–d shows box plots of the RTE values corresponding to fibrosis stage and includes the healthy volunteer (HV) group. The Mean decreased with increasing fibrosis

score (Jonckheere–Terpstra test, $p < 0.0001$). SD, Area, and Complexity increased with increasing fibrosis score (Jonckheere–Terpstra test, $p < 0.0001$). The significant differences between each fibrosis stage were as follows: HV versus F3 and F4, F1 versus F3 and F4, and F2 versus F4 at every parameter; HV versus F2 at Mean, SD, and Area; F1 versus F2 at Mean; F2 versus F3 at Mean; F3 versus F4 at Complexity (Tukey–Kramer test, $p < 0.05$) No significant difference was found between the chronic hepatitis activity grades with same fibrosis stage at all parameters (Tukey–Kramer test).

Relationship between real-time tissue elastography and liver stiffness

Figure 4a–d, shows linear regression analysis of the values obtained by RTE compared to the liver stiffness values (kPa) obtained by transient elastography (Fibroscan). Simple regression analyses indicated that Mean, SD, Area, and Complexity were all significantly correlated with liver stiffness measured by Fibroscan (Mean: $r = -0.585$, $p < 0.001$; SD: $r = 0.425$, $p < 0.001$; Area: $r = 0.590$, $p < 0.001$; Complexity: $r = 0.532$, $p < 0.001$).

Relationship between real-time tissue elastography and platelet count, APRI, and other laboratory parameters

Simple regression analyses indicated that all Mean, SD, Area, and Complexity values were significantly correlated with the platelet count (Mean: $r = 0.432$, $p < 0.001$; SD: $r = -0.332$, $p = 0.001$; Area: $r = -0.402$, $p < 0.001$; Complexity: $r = -0.393$, $p < 0.001$). In addition, simple regression analyses indicated that Mean, SD, Area, and Complexity were all significantly correlated with APRI (Mean: $r = -0.442$, $p < 0.001$; SD: $r = 0.373$, $p < 0.001$; Area: $r = 0.425$, $p < 0.001$; Complexity: $r = 0.418$, $p < 0.001$). Furthermore, the correlation coefficient was significant for prothrombin time (Mean: $r = -0.404$, $p < 0.001$; SD: $r = 0.343$, $p < 0.005$; Area: $r = 0.435$, $p < 0.001$; Complexity: $r = 0.440$, $p < 0.001$), while no significant correlation was found for the four image features and total bilirubin, age, BMI, or alanine aminotransferase.

Diagnostic value of real-time tissue elastography and transient elastography

Figure 5 shows the ROC curves of RTE parameters for no significant fibrosis (F0–1) and cirrhosis (F4) in ninety-six patients who were also examined successfully by transient elastography. The AUCs for the stage of no significant fibrosis (F0–1) were 0.89, 0.81, 0.87, and 0.81 for Mean, SD, Area, and Complexity, respectively. The AUCs for severe fibrosis (≥F3) were 0.93, 0.84, 0.91, and 0.86 for Mean, SD, Area, and Complexity, respectively. The AUCs for cirrhosis (F4) were 0.91, 0.84, 0.91, and 0.93 for Mean, SD, Area, and Complexity, respectively. In transient elastography (Fibroscan), the AUCs were 0.92, 0.95, and 0.95 for stages F0–1, ≥F3s and F4, respectively. The corresponding sensitivities, specificities, and positive and negative predictive values are detailed in Table 2.

Discussion

Recently, various techniques based on ultrasound or magnetic resonance imaging have been developed to quantify

Table 2 Cutoff values of real-time tissue elastography (image features) and transient elastography for the diagnosis of fibrosis stages (*F*)

	$F = 0$–1	$F \geq 3$	$F = 4$
Mean (AUC)	0.89	0.93	0.91
Cutoff (a.u.)	110.1	106.9	101.5
Sensitivity (%)	84.1	82.8	85.7
Specificity (%)	82.7	85.1	82.9
Positive predictive value (%)	80.4	70.6	46.2
Negative predictive value (%)	86.0	91.9	97.1
SD (AUC)	0.81	0.84	0.84
Cutoff (a.u.)	61.2	63.0	65.7
Sensitivity (%)	70.5	75.9	78.6
Specificity (%)	73.1	77.6	79.3
Positive predictive value (%)	68.9	59.5	39.3
Negative predictive value (%)	74.5	88.1	95.6
Area (AUC)	0.87	0.91	0.91
Cutoff (%)	25.8	29.5	33.7
Sensitivity (%)	81.8	79.3	85.7
Specificity (%)	80.8	80.6	86.6
Positive predictive value (%)	78.3	63.9	52.2
Negative predictive value (%)	79.6	90.0	97.3
Complexity (AUC)	0.81	0.86	0.93
Cutoff (a.u.)	23.2	24.9	27.8
Sensitivity (%)	77.3	79.3	85.7
Specificity (%)	75.0	80.6	87.8
Positive predictive value (%)	72.3	63.9	54.5
Negative predictive value (%)	79.6	90.0	97.3
Transient elastography (AUC)	0.92	0.95	0.95
Cutoff (kPa)	10.1	13.3	16.3
Sensitivity (%)	88.6	89.7	85.7
Specificity (%)	86.5	86.6	85.4
Positive predictive value (%)	84.8	74.3	50.0
Negative predictive value (%)	90.0	95.1	97.2

AUC the area under the receiver operating characteristic curves, *a.u.* arbitrary units

liver stiffness, and thereby liver fibrosis, noninvasively. Among them, transient elastography (Fibroscan) has been used most frequently worldwide and has become established in clinical practice to detect advanced fibrosis without liver biopsy, although several limitations and disadvantages of the modality have been discussed [8, 24]. Another novel imaging modality is magnetic resonance elastography (MRE). The technique typically is added to a conventional MR examination of the upper abdomen [25]. A pneumatic or electromechanical driver is placed in contact with the abdominal wall and is used to generate propagating mechanical waves in the liver at frequencies between 40 and 120 Hz. Although MRE was shown to be superior to APRI and transient elastography for determining the stage of fibrosis in patients with various underlying liver diseases [26], MRE cannot be performed on an iron-overloaded liver because of noise. In addition, MRE takes a longer time and costs more than the ultrasound-based elastographies [2].

We paid attention in our analysis to the pattern change of RTE color images according to the progression of fibrosis. Normal or minimally fibrotic liver exhibited a homogeneous RTE image that was colored light green (Fig. 2a). According to the progression of liver fibrosis, the homogeneous pattern transited to a patchy pattern consisting of a blue-colored area (Fig. 2c), which may suggest a collapse of homogeneity. In the present study, for semi-quantification of the RTE image, we used a histogram and binary image produced using an exclusive software program that was developed by Hitachi Medical. This is the first report demonstrating the utility of Mean, SD, Area, and Complexity as RTE parameters. We speculate that Mean and Area may directly represent liver elasticity, while SD and Complexity may imply the collapse of the uniform architecture of the liver parenchyma concomitant with progressing hepatic fibrosis (Figs. 3, 5).

After the report by Friedrich-Rust et al. [21] other investigators criticized the intraobserver variability and the lack of interobserver agreement in hepatic RTE [27–29]. In general practice, an operator presses lightly on the surface of the liver through the skin with a transducer when the elastogram is generated. Thus, the pressure generated by the operator's compression is assumed to influence both the image of elasticity and the resulting elasticity score. To avoid this source of error, we used here the latest and most sensitive probe that was produced by Hitachi Medical and did not require extra external stress. Accordingly, we were able to improve the acquisition of the color image representing the distortion of liver tissue under the heartbeat or abdominal aorta. We also adopted ten individual frames for semi-quantitative analysis. On the other hand, Saftoiu et al. and Gulizia et al. have proposed that the ROI should include the surrounding tissues, such as adipose tissue, diaphragm, and intercostal muscles, in order to clearly compare and distinguish the strain between the liver and these organs [27, 30]. However, we placed the ROI inside the liver at 5 mm below the surface of the liver, because the new probe used in this study is sensitive and the deep attenuation of the ultrasound image could be disregarded. We avoided including the liver surface inside the ROI because the liver surface is hard and therefore is assessed as a harder area, influencing the histogram analysis. Recently, Tatsumi et al. [31] also reported the results of RTE using the ROI inside the liver in a similar fashion to our study.

We note that all four image features of RTE, comprising Mean, SD, Area, and Complexity, were significantly correlated with the kPa value obtained by Fibroscan [8, 11–13]. In particular, Mean and Area had a high correlation. In addition, the AUC values were similar between RTE and Fibroscan. Mean and Area were highly accurate for the diagnosis of significant fibrosis (i.e., >F0–1) and for the diagnosis of cirrhosis (F4). Although the performance of Fibroscan has been demonstrated in many studies to have high accuracy [4, 8], the machine is used solely for elasticity measurements. In contrast, with the new equipment used in the present study, RTE can be used simultaneously with conventional B-mode ultrasonography. Moreover, as reported by Obara et al. [32], liver stiffness measurement by Fibroscan was unsuccessful in 5.3% of Japanese cases of chronic liver disease, similar to our experience in the present study (5.0%). Thus, RTE is considered to be superior to Fibroscan at points where measurements by Fibroscan are difficult to perform in obese patients and are impossible to perform in patients with ascites [32, 33], and where RTE images are unaffected by steatosis, as suggested previously by Friedrich-Rust et al. [29]. Furthermore, because Fibroscan measures liver stiffness between 25 and 65 mm below the surface of the skin [10], knowledge of the relative thickness of the liver is necessary for the measurements.

The diagnostic performance of RTE is similar to that of other noninvasive laboratory tests, such as the FibroTest (BioPredictive, Paris, France), APRI, and the Forns score reported in the literature [4, 8]. The FibroTest is based on five serological parameters; bilirubin, gamma-glutamyl transpeptidase (GGT), apolipoprotein A1, α2-macroglobulin, and haptoglobin. While the diagnostic accuracy was high (AUC 0.87) for significant fibrosis (METAVIR, ≥F2), the FibroTest costs more than APRI and the Forns score, and needs two uncommon parameters [34]. In APRI, using the cutoffs proposed by Wai et al. [5], approximately 50% of patients could be correctly classified as having cirrhosis without a liver biopsy5. With the Forns' index, the AUC for the prediction of significant fibrosis (Scheuer classification, ≥F2) was 0.86 in the test set and 0.81 in the validation set [35]. It is, however, known that the determination of the

severity of liver fibrosis by serum markers is confounded by acute inflammation, hemolysis, cholestasis, and renal failure [4, 5, 34, 35]. Castera et al. [11] compared the performance of transient elastography with that of the FibroTest, APRI, and liver biopsy for the assessment of liver fibrosis in a large number of patients with hepatitis C. Interestingly, they reported that the best performance was achieved by a combination of transient elastography with the FibroTest [11]. Friedrich-Rust et al. reported that the best diagnostic accuracy was obtained by combining the variables used for the calculation of the RTE elasticity score with the platelet count and GGT [18]. Thus, RTE, in combination with serological parameters, can further improve the accuracy of differentiating fibrosis stages.

One of the major limitations of the present study was that the number of patients with F1 was higher than the number of those with the other stages, because most of our patients received liver biopsy prior to interferon treatment. However, our study compared the performance of RTE with that of transient elastography in the same patients. Although the AUC for RTE in this study was higher than that in the studies by Friedrich-Rust et al. [21, 29], the AUC for transient elastography was approximately equivalent to that in one of these studies [29].

In the METAVIR and Desmet's histological scoring systems, cirrhosis is classified as a single category (i.e., F4) [22, 23]. However, the degree of fibrosis; for example, the content of collagen and extracellular matrix materials that may be closely associated with the function of hepatocytes and portal hypertension, may vary among patients with cirrhosis. Foucher et al. [36] reported that the kPa measured by transient elastography in cirrhotic patients correlated well with clinical parameters indicating the severity of cirrhosis; 27.5 kPa was the cutoff value for the presence of esophageal varices stage 2 or 3, 37.5 kPa for liver function Child B or C, 49.1 kPa for a past history of ascites, and 62.7 kPa for esophageal variceal bleeding. Thus, because cirrhosis can be staged in greater detail with clinical relevance based on liver stiffness with RTE, RTE may be useful for this staging of cirrhosis and for detecting and assessing the risk of cirrhotic complications [36].

In summary, we have shown a convenient and noninvasive procedure, RTE, for the visual assessment of liver stiffness. The performance of RTE compares favorably with that of transient elastography (Fibroscan) for detecting the presence of significant liver fibrosis in patients with chronic hepatitis C. We suggest that RTE could be used as a routine imaging method to evaluate the degree of liver fibrosis in patients with liver disease. Future studies of larger patient cohorts will be necessary for the validation of the four RTE parameters, and the combination of these parameters will enable improvement of accuracy in assessing hepatic fibrosis.

Acknowledgments We thank Ms. Akiko Tonomura and Mr. Junji Warabino, Hitachi Medical Co., for the technical support for RTE. Hiroyasu Morikawa was supported by a research grant from Osaka City University (2009). Norifumi Kawada was supported by Research on Hepatitis, Health and Labour Science Research Grants from the Ministry of Health, Labour and Welfare of Japan (2008–2009) and by a Thrust Area Research Grant from Osaka City University (2008–2009).

References

1. Global surveillance and control of hepatitis C. Report of a WHO Consultation organized in collaboration with the Viral Hepatitis Prevention Board, Antwerp, Belgium. J Viral Hepat. 1999;6:35–47.
2. Manns MP, McHutchison JG, Gordon SC, Rustgi VK, Shiffman M, Reindollar R, et al. Peginterferon alfa-2b plus ribavirin compared with interferon alfa-2b plus ribavirin for initial treatment of chronic hepatitis C: a randomised trial. Lancet. 2001;358:958–65.
3. Sporea I, Popescu A, Sirli R. Why, who and how should perform liver biopsy in chronic liver diseases. World J Gastroenterol. 2008;14:3396–402.
4. Manning DS, Afdhal NH. Diagnosis and quantitation of fibrosis. Gastroenterology. 2008;134:1670–81.
5. Wai CT, Greenson JK, Fontana RJ, Kalbfleisch JD, Marrero JA, Conjeevaram HS, et al. A simple noninvasive index can predict both significant fibrosis and cirrhosis in patients with chronic hepatitis C. Hepatology. 2003;38:518–26.
6. Sandrin L, Tanter M, Gennisson JL, Catheline S, Fink M. Shear elasticity probe for soft tissues with 1D transient elastography. IEEE Trans Ultrason Ferroelectr Freq Control. 2002;49:436–46.
7. Ganne-Carrié N, Ziol M, de Ledinghen V, Douvin C, Marcellin P, Castera L, et al. Accuracy of liver stiffness measurement for the diagnosis of cirrhosis in patients with chronic liver diseases. Hepatology. 2006;44:1511–7.
8. Pinzani M, Vizzutti F, Arena U, Marra F. Technology Insight: noninvasive assessment of liver fibrosis by biochemical scores and elastography. Nat Clin Pract Gastroenterol Hepatol. 2008;5:95–106.
9. Yeh WC, Li PC, Jeng YM, Hsu HC, Kuo PL, Li ML, et al. Elastic modulus measurements of human liver and correlation with pathology. Ultrasound Med Biol. 2002;28:467–74.
10. Sandrin L, Fourquet B, Hasquenoph JM, Yon S, Fournier C, Mal F, et al. Transient elastography: a new noninvasive method for assessment of hepatic fibrosis. Ultrasound Med Biol. 2003;29:1705–13.
11. Castéra L, Vergniol J, Foucher J, Le Bail B, Chanteloup E, Haaser M, et al. Prospective comparison of transient elastography, Fibrotest, APRI, and liver biopsy for the assessment of fibrosis in chronic hepatitis C. Gastroenterology. 2005;128:343–50.
12. Ziol M, Handra-Luca A, Kettaneh A, Christidis C, Mal F, Kazemi F, et al. Noninvasive assessment of liver fibrosis by measurement of stiffness in patients with chronic hepatitis C. Hepatology. 2005;41:48–54.
13. Friedrich-Rust M, Ong MF, Martens S, Sarrazin C, Bojunga J, Zeuzem S, et al. Performance of transient elastography for the staging of liver fibrosis: a meta-analysis. Gastroenterology. 2008;134:960–74.
14. Arena U, Vizzutti F, Corti G, Ambu S, Stasi C, Bresci S, et al. Acute viral hepatitis increases liver stiffness values measured by transient elastography. Hepatology. 2008;47:380–4.
15. Nitta N, Yamakawa M, Shiina T. Tissue elasticity imaging based on combined autocorrelation method and 3D tissue model. In: Proceedings of the IEEE Ultrasonics Symposium. Savoy, Ill:

Institute of Electrical and Electronics Engineers Ultrasonics, Ferroelectrics, and Frequency Control Digital Archive 1998, vol. 2, p. 1447–50.
16. Yamakawa M, Shiina T. Strain estimation using the extended combined autocorrelation method. Jpn J Appl Phys. 2001;40:3872–6.
17. Itoh A, Ueno E, Tohno E, Kamma H, Takahashi H, Shiina T, et al. Breast disease: clinical application of US elastography for diagnosis. Radiology. 2006;239:341–50.
18. Tohno E, Ueno E. Current improvements in breast ultrasound, with a special focus on elastography. Breast Cancer. 2008;15:200–4.
19. Tsutsumi M, Miyagawa T, Matsumura T, Kawazoe N, Ishikawa S, Shimokama T, et al. The impact of real-time tissue elasticity imaging (elastography) on the detection of prostate cancer: clinicopathological analysis. Int J Clin Oncol. 2007;12:250–5.
20. Uchida H, Hirooka Y, Itoh A, Kawashima H, Hara K, Nonogaki K, et al. Feasibility of tissue elastography using transcutaneous ultrasonography for the diagnosis of pancreatic diseases. Pancreas. 2009;38:17–22.
21. Friedrich-Rust M, Ong MF, Herrmann E, Dries V, Samaras P, Zeuzem S, et al. Real-time elastography for noninvasive assessment of liver fibrosis in chronic viral hepatitis. AJR Am J Roentgenol. 2007;188:758–64.
22. Desmet VJ, Gerber M, Hoofnagle JH, Manns M, Scheuer PJ. Classification of chronic hepatitis: diagnosis, grading and staging. Hepatology. 1994;19:1513–20.
23. The French Metavir Cooperative Study Group. Intraobserver and interobserver variations in liver biopsy interpretation in patients with chronic hepatitis C. Hepatology. 1994;20:15–20.
24. Bonekamp S, Kamel I, Solga S, Clark J. Can imaging modalities diagnose and stage hepatic fibrosis and cirrhosis accurately? J Hepatol. 2009;50:17–35.
25. Muthupillai R, Lomas DJ, Rossman PJ, Greenleaf JF, Manduca A, Ehman RL. Magnetic resonance elastography by direct visualization of propagating acoustic strain waves. Science. 1995;269:1854–7.
26. Huwart L, Sempoux C, Vicaut E, Salameh N, Annet L, Danse E, et al. Magnetic resonance elastography for the noninvasive staging of liver fibrosis. Gastroenterology. 2008;135:32–40.
27. Săftoiu A, Gheonea DI, Ciurea T. Hue histogram analysis of real-time elastography images for noninvasive assessment of liver fibrosis (letter). AJR Am J Roentgenol. 2007;189:W232–3.
28. Ferraioli G, Gulizia R, Filice C. Real-time elastography in the assessment of liver fibrosis (letter). AJR Am J Roentgenol. 2007;189:W170.
29. Friedrich-Rust M, Schwarz A, Ong M, Dries V, Schirmacher P, Herrmann E, et al. Real-time tissue elastography versus FibroScan for noninvasive assessment of liver fibrosis in chronic liver disease. Ultraschall Med. 2009;30:478–84.
30. Gulizia R, Ferraioli G, Filice C. Open questions in the assessment of liver fibrosis using real-time elastography. AJR Am J Roentgenol. 2008;190:W370–1.
31. Tatsumi C, Kudo M, Ueshima K, Kitai S, Ishikawa E, Yada N, et al. Non-invasive evaluation of hepatic fibrosis for type C chronic hepatitis. Intervirology. 2010;53:76–81.
32. Obara N, Ueno Y, Fukushima K, Nakagome Y, Kakazu E, Kimura O, et al. Transient elastography for measurement of liver stiffness measurement can detect early significant hepatic fibrosis in Japanese patients with viral and nonviral liver diseases. J Gastroenterol. 2008;43:720–8.
33. Ogawa E, Furusyo N, Toyoda K, Takeoka H, Otaguro S, Hamada M, et al. Transient elastography for patients with chronic hepatitis B and C virus infection: non-invasive, quantitative assessment of liver fibrosis. Hepatol Res. 2007;37:1002–10.
34. Imbert-Bismut F, Ratziu V, Pieroni L, Charlotte F, Benhamou Y, Poynard T, et al. Biochemical markers of liver fibrosis in patients with hepatitis C virus infection: a prospective study. Lancet. 2001;357:1069–75.
35. Forns X, Ampurdanès S, Llovet JM, Aponte J, Quintó L, Martínez-Bauer E, et al. Identification of chronic hepatitis C patients without hepatic fibrosis by a simple predictive model. Hepatology. 2002;36:986–92.
36. Foucher J, Chanteloup E, Vergniol J, Castéra L, Le Bail B, Adhoute X, et al. Diagnosis of cirrhosis by transient elastography (FibroScan): a prospective study. Gut. 2006;55:403–8.